Uveal melanoma

Martine J. Jager[1] ✉, Carol L. Shields[2], Colleen M. Cebulla[3], Mohamed H. Abdel-Rahman[3,4], Hans E. Grossniklaus[5,6], Marc-Henri Stern[7], Richard D. Carvajal[8], Rubens N. Belfort[9], Renbing Jia[10], Jerry A. Shields[2] and Bertil E. Damato[11]

Abstract | Uveal melanoma (UM) is the most common primary intraocular malignancy in adults. UMs are usually initiated by a mutation in *GNAQ* or *GNA11*, unlike cutaneous melanomas, which usually harbour a *BRAF* or *NRAS* mutation. The annual incidence in Europe and the USA is ~6 per million population per year. Risk factors include fair skin, light-coloured eyes, congenital ocular melanocytosis, ocular melanocytoma and the *BAP1*-tumour predisposition syndrome. Ocular treatment aims at preserving the eye and useful vision and, if possible, preventing metastases. Enucleation has largely been superseded by various forms of radiotherapy, phototherapy and local tumour resection, often administered in combination. Ocular outcomes are best with small tumours not extending close to the optic disc and/or fovea. Almost 50% of patients develop metastatic disease, which usually involves the liver, and is usually fatal within 1 year. Although UM metastases are less responsive than cutaneous melanoma to chemotherapy or immune checkpoint inhibitors, encouraging results have been reported with partial hepatectomy for solitary metastases, with percutaneous hepatic perfusion with melphalan or with tebentafusp. Better insight into tumour immunology and metabolism may lead to new treatments.

Congenital ocular melanocytosis
A congenital periocular or ocular pigment condition.

Photopsia
Flashes of light.

Enucleation
Removal of the eye.

Uveal melanoma (UM) is a rare disease that is very different from its cutaneous counterpart[1]. UMs arise from melanocytes in the uvea, which comprises the pigmented tissues of the iris (in the anterior chamber of the eye), and ciliary body and choroid (in the posterior chamber of the eye; FIG. 1). More than 90% of UMs involve the choroid, with only 6% being confined to the ciliary body and 4% to the iris[2]. Most patients present between the ages of 50 years and 70 years; occurrence before adulthood is rare[3]. The disease is usually unilateral. Risk factors for developing UM include fair skin, light-coloured eyes, congenital ocular melanocytosis, melanocytoma and the *BAP1*-tumour predisposition syndrome[4]. A role for ultraviolet (UV) radiation exposure in UM has been suggested, as in cutaneous melanoma, but is unlikely to be involved in posterior UMs owing to the very low mutation burden and absence of a UV mutational signature in UM[5–8]; the cornea, lens and vitreous effectively remove most UV radiation such that very little reaches the choroid[9]. However, tumour initiation has a predilection for the macula, where light is focused, suggesting a role for non-UV wavelengths[10]. UMs of the iris are located in front of the lens, and may be under the influence of UV-induced DNA damage (BOX 1).

UMs usually present with symptoms such as blurred or distorted vision, visual field loss or photopsia; ~30% are asymptomatic and detected on routine examination (such as regular check-up or diabetic retinopathy screening)[11]. Ocular treatment aims to conserve the eye and useful vision and consists of various forms and combinations of radiotherapy, phototherapy and local resection, reserving enucleation for advanced cases. Despite treatment of the primary tumour, ~50% of patients with UM will develop metastatic disease (usually via haematogenous spread)[12,13]. Currently, effective therapies to prevent the development of metastases are not available, but early treatment of indeterminate lesions may help to prevent the development of lethal UM[14]. Metastases from UM respond poorly to chemotherapy or targeted therapy and are usually fatal within 1 year of the onset of symptoms. Long-term survival is rare except in patients with isolated liver metastases that are amenable to surgical resection. Unlike cutaneous melanoma metastases, UM metastases generally do not respond to immune checkpoint inhibitors. However, encouraging results with other immunotherapy strategies are emerging.

Choroidal naevi (BOX 2) and UM almost all carry a driver mutation in a *GNA* family gene[15–17], such as *GNA11* and *GNAQ*, which encode guanine nucleotide-binding protein Gα subunits of the $G\alpha_q$ family. Recent multi-omic analyses have defined molecular UM subsets, which differ in their genetic aberrations, methylation pattern, gene expression profile (GEP), and metabolomic and immunological characteristics[5,18–20] (TABLE 1). Prognostically favourable type A and B UMs are

✉*e-mail: m.j.jager@lumc.nl*

https://doi.org/10.1038/s41572-020-0158-0

Author addresses

[1]Department of Ophthalmology, Leiden University Medical Center, Leiden, The Netherlands.
[2]Ocular Oncology Service, Wills Eye Hospital, Thomas Jefferson University, Philadelphia, PA, USA.
[3]Havener Eye Institute, Department of Ophthalmology and Visual Science, The Ohio State University Wexner Medical Center, Columbus, OH, USA.
[4]Division of Human Genetics, Department of Internal Medicine, The Ohio State University Columbus, Columbus, OH, USA.
[5]Department of Ophthalmology, Emory University, Atlanta, GA, USA.
[6]Department of Pathology and Laboratory Medicine, Emory University Atlanta, GA, USA.
[7]Inserm U830, DNA Repair and Uveal Melanoma (D.R.U.M.), Equipe labellisée par la Ligue Nationale Contre le Cancer, Institut Curie, PSL Research University, Paris, France.
[8]Department of Medicine, Columbia University Medical Center, New York, NY, USA.
[9]Department of Ophthalmology and Visual Sciences, Federal University of São Paulo, São Paulo, Brazil.
[10]Department of Ophthalmology, Ninth People's Hospital, Shanghai Jiao Tong University School of Medicine, Shanghai, China.
[11]Nuffield Department of Clinical Neurosciences, University of Oxford, West Wing, John Radcliffe Hospital, Oxford, UK.

characterized by disomy 3, a class 1 GEP, and with either two (type A) or more (type B) copies of chromosome 8q. Type A UMs often have a mutation in *EIF1AX* (encoding eukaryotic translation initiation factor 1A X-linked (eIF1A)), whereas type B UMs may have a mutation in *SF3B1* (encoding splicing factor 3B subunit 1A)[7,21]. By contrast, prognostically unfavourable type C and D UMs are highly lethal; these UMs show monosomy 3, a class 2 GEP, inactivation of *BAP1* (encoding BRCA1-associated protein 1; located on chromosome 3), multiple copies of chromosome 8q and, in type D, an inflammatory phenotype[18,20,22–24].

Dysplastic naevi
Large and irregularly shaped cutaneous moles.

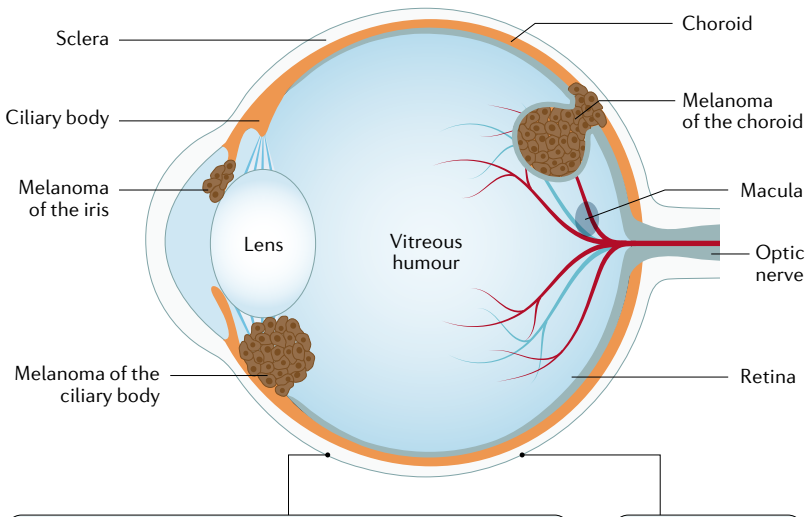

Fig. 1 | **Development of UM.** Uveal melanomas (UMs) arise from melanocytes in the pigmented uveal tissues of the eye; the uvea is made up of the iris, ciliary body and choroid. Individuals at increased risk of developing UM include those 50–70 years of age, and those with a fair skin colour and a sensitivity to sunburn, a light iris colour, congenital ocular melanocytosis (a congenital ocular pigmentary condition) or melanocytoma. Individuals with a family history of cutaneous melanoma and UM are also at risk, as are those with the *BAP1*-tumour predisposition syndrome. Some UMs (30%) are asymptomatic and are discovered on routine examination.

In this Primer, we describe the biological and clinical features of UM, focusing on posterior UM, as these share many characteristics and differ from anterior UMs. We discuss the current ophthalmological and systemic management of patients with this disease. Although treatment of the primary tumour is usually quite effective, therapies to prevent and treat the (currently) deadly metastases are urgently needed. We describe the newest developments with regard to personalized treatments and immunotherapy, which may ultimately lead to effective treatment of tumour metastases.

Epidemiology

Although some studies have shown that men and women are affected in equal numbers, others suggest a slight preponderance of UM in men[25]. The incidence of UM varies from <1 to >9 per million population per year[26]. In Europe, the incidence varies by region, with a south-to-north increasing gradient that is reflected in a minimum incidence of <2 per million population in Spain and southern Italy, and a maximum of >8 per million population in Ireland, Norway and Denmark[25,27]. The incidence in Australia and New Zealand is similar to that in northern Europe, 9.8 and 9 per million population per year, respectively[28,29]. The incidence is low in Asian countries/jurisdictions such as South Korea (0.4 per million per year)[30] and Japan (0.6 per million per year)[31], as well as in Africa (0.3 per million per year)[32]. Factors associated with an increased risk of UM in these populations include fair skin, light eye colour (blue and grey iris colour) and an increased tendency to sunburn; blonde or red hair has not consistently been reported as a significant risk factor[33,34]. Patients with UM also have an increased frequency of dysplastic naevi, cutaneous melanomas and a positive family history of this malignancy[35–37]. The 5-year and 15-year disease-related mortality of UM is ~30% and ~45%, respectively[12].

Genetic risk factors

Thus far, only a few studies have looked at the genetic basis of UM, uncovering high-risk and low-risk loci worthy of further investigation. For low-risk loci, a study of single nucleotide polymorphisms (SNPs) known to be risk variants for cutaneous melanoma in a series of 272 patients with UM and 1,782 controls showed a significant association between UM risk and SNPs in the pigmentation genes *HERC2*, *OCA2* and *IRF4* (REF.[38]). This finding is consistent with the known association of blue eyes and fair skin with UM[39]. A subsequent genome-wide association study (GWAS) study comparing 535 patients with UM and 585 healthy controls confirmed the association between SNPs in pigmentation genes and UM[40]. The GWAS analysis also revealed a new candidate locus at chromosome 5p15.33 in the region that includes the genes *TERT* (encoding telomerase reverse transcriptase) and *CLPTM1L* (encoding cleft lip and palate transmembrane protein 1-like protein)[40]. Risk variants from this region were positively associated with a higher expression of *CLPTM1L* in UM, which purportedly contributes

Box 1 | **Uveal melanoma of the iris**

Owing to its greater visibility, iris melanoma is typically diagnosed at an earlier stage than ciliary body and choroidal melanoma; it has a lower histological grade and the lowest incidence of metastasis, which is thought to reflect its small tumour burden[327]. In addition to light eye colour, welding may increase the risk of developing iris melanoma, for reasons that are unclear[64]. Iris melanomas are more frequent in the inferior quadrant of the iris[2], a location that is prone to develop naevi and receives greater ultraviolet (UV) radiation exposure than other parts of the eye[64]. Although the overall frequency of uveal melanomas (UMs) is low in young people (<21 years of age, most presenting at 15–20 years of age), this population has a relatively higher frequency of iris melanoma (12–41% of UMs) than in adults (~4–8%)[7,328,329]. Genetically, iris melanomas can resemble ciliary body and choroidal melanoma[330,331], or cutaneous melanoma[332]. A gene expression profile study found that one-third of iris melanomas have a high-risk class 2 molecular signature[333], despite their low rate of metastasis.

Iris melanomas are diagnosed on clinical examination, gonioscopy and iris photography, and high-resolution anterior segment ultrasonography. Growth of the lesion is a hallmark of malignant transformation, which is also associated with age ≤40 years, hyphaema (pooling of blood inside the anterior chamber of the eye), inferior location of the tumour, diffuse extent of tumour, ectropion uvea (the presence of pigment epithelium on the anterior surface of the iris) and feathery margins[334]. Other important features include tumour nodule, vascularity, tumour seeding, sectoral cataract and secondary glaucoma. Staging is performed using the American Joint Committee on Cancer tumour–node–metastasis staging for iris tumours[335].

Iris melanoma is treated by surgical excision, brachytherapy, proton beam therapy or enucleation[336,337]. Fine-needle or vitrector-assisted aspiration biopsy may be performed to confirm the diagnosis and provide tissue for genetic testing[338,339]. During brachytherapy, placing an amniotic membrane graft under the plaque can protect the cornea and reduce discomfort. Glaucoma secondary to iris melanoma may be due to tumour involvement in the angle, hyphaema and neovascularization of the angle. Filtering surgery or minimally invasive glaucoma surgery should be avoided[234,340]. Follow-up with a medical oncologist for systemic tumour surveillance is recommended.

to RAS-dependent transformation and tumorigenesis[41]. Additionally, genetic risk loci may be found by analysing exceptional cases; when characterizing outlier responders to immune checkpoint therapy, deleterious germline mutations of *MBD4* were found in four patients with UM[42,43]. Inactivation of *MBD4* in tumours leads to a hypermutator phenotype, even in UM with its otherwise low mutational load.

For high-risk loci, the Cancer Genome Atlas (TCGA) project has identified rare germline mutations in seven different cancer genes[18,44], of which *BAP1* shows strong evidence for association with hereditary predisposition to UM[45]. Although the frequency of *BAP1* germline mutations is 1–2% in the overall population of patients with UM[44,46,47], it increases to 18–22% in those with familial occurrence of UM (FUM)[48,49]. FUM is defined as the occurrence of UM in two or more individuals in the same blood line, and represents 0.6% of all UMs[50]; in FUM, the UM is usually unilateral[48]. In addition to *BAP1*, germline mutations in other known cancer genes (such as *MLH1*, *PALB2* and *SMARCE1*) are observed in an additional 9% of patients with FUM[51,52]. Other genomic analyses have revealed sporadic associations with several other genes, such as *BRCA1* (REFS[51,53]), *BRCA2* (REFS[54,55]), *FLCN*[56,57], *MSH6* (REFS[51,58]), and *CHEK2* (REF.[51]). For genes other than *BAP1*, evidence for association with UM ranges from moderate (*MLH1* and *PALB2*) to limited (all other genes) due to the rarity of UM and the significant genetic and phenotypic heterogeneity of the disease[51].

Approximately 12% of patients with UM have a strong personal and/or family history of cancer[50,59]. A wide variety of non-ocular second primary cancers have been reported, including cutaneous melanoma[4,36,48,60], gastrointestinal and urinary tract cancers, breast cancer, non-Hodgkin lymphoma[59,61–63] and multiple myeloma. UM may occur as part of the *BAP1*-tumour predisposition syndrome, which is associated with the development of melanocytic cutaneous tumours, mesothelioma and renal cell carcinoma. Other malignancies that have been linked to this syndrome include meningioma, cutaneous basal cell carcinoma and cholangiocarcinoma[4].

Environmental risk factors

Epidemiological studies have identified welding as an environmental risk factor for UM[64,65]. The risk from welding is more complex than just UV exposure, as it includes visible and infrared radiation, and frequently co-occurs with other potential risk factors such as chemical exposure[64]. Indeed, associated chemical risk factors include asbestos, antifreeze, formaldehyde and pesticides[65]. Environmental exposure to chemicals may play a part in patients with a *BAP1*-germline mutation. Mice with an inducible *BAP1* mutation develop more malignancies in response to asbestos, associated with an increased inflammatory response[66]. Similarly, patients with mesothelioma harbouring *BAP1* mutations show a higher sensitivity to asbestos[67].

Other epidemiological risk factors include the use of sunlamps, cumulative intense sun exposure and commercial cooking[64,65]. Despite publicity in the media, no scientific evidence links UM to the use of mobile phones[68]. In the USA, unexplained clusters of UM have occurred in Auburn, AL[69] and Huntersville, NC[70].

Mechanisms/pathophysiology

Genetic variants associated with an elevated risk of developing UM, including variants of pigmentation genes, are likely to account for the epidemiological trends of UM. However, the roles of the different types of melanin in early malignant transformation are under investigation. Mechanistically, we can deduce a link between light eye colour and higher propensity of developing UM. Blue or grey irises are associated with phaeomelanin (yellow–brown pigment), whereas brown irises are associated with eumelanin (black–brown pigment)[71]. Melanocytes with reduced functional OCA2, which is likely to be involved in the rate limiting step of melanin synthesis, show defective eumelanin synthesis, but normal phaeomelanin synthesis[72,73] (FIG. 2). The UM themselves may vary from amelanotic, lightly pigmented to heavily pigmented. Amelanocytic tumours are associated with catalytically inactive or less active tyrosinase[74]. Electron microscopy studies of amelanotic tumours have shown abnormal morphology and characteristics of the melanosomes, with preserved phaeomelanin and loss of eumelanin in the melanosomes[75]. Occasionally, tumours are partially amelanotic and partially pigmented.

Malignant transformation

Highly recurrent mutations in UM strongly support the notion that subsequent malignant transformation in choroidal melanocytes is driven by the combination of two main events. These events are an alteration in the $G\alpha_q$

Box 2 | **Choroidal naevi**

The choroidal naevus is the most common intraocular tumour[341] (usually <1.5 mm in thickness); it results from outgrowth of melanocytes derived from the neural crest. Naevi are uncommon in children, and the prevalence is 1.4–6.5% in adults, increasing with age[342]. Prevalence is higher in white individuals than in those of Hispanic, African or Asian descent. Most choroidal naevi are asymptomatic, but can become symptomatic owing to, for example, secondary serous foveal detachment, photoreceptor degeneration or subretinal choroidal neovascularization. Most naevi are located posterior to the equator, are largely brown in colour but can also be yellow (amelanotic) or mixed brown and yellow (melanotic–amelanotic). The overlying retinal pigment epithelium may undergo changes such as the development of drusen (yellow, lipid-rich deposits under the retina), atrophy or hyperplasia. Genetically, most naevi are already characterized by a *GNAQ* or *GNA11* mutation[15]. Histologically, naevi can be thick or thin, and with vessels inside the naevus or at its border. Three different cell types can be distinguished: plump polyhedral naevus cells, slender spindle cells and balloon cells.

Ultrasonography is used to measure the naevus and to differentiate a naevus from a melanoma; naevi have high internal reflectivity on diagnostic A-scan ultrasonography, whereas melanomas have lower internal reflectivity. Fluorescein angiography can be applied to determine 'hot spots', which are bright pinpoint hyperfluorescent foci, and leakage of fluorescein, which are signs of malignancy. Spectral domain optical coherence tomography (SD-OCT), especially with enhanced depth imaging mode, may show choriocapillaris thinning overlying the naevus, retinal pigment epithelium atrophy and photoreceptor loss. Growth of a naevus may be a sign of malignant transformation into a choroidal melanoma. The annual rate of malignant transformation of a naevus into a melanoma in white Americans has been calculated to be 1 in 8,845 individuals[85]. Risk factors for naevus transformation include thickness >2 mm, diameter >5 mm, subretinal fluid, symptoms, orange pigment on the tumour surface and acoustic hollowing of the tumour on ultrasonography, which is an echogenically 'empty' (or dark) appearance of the tumour on B-scan ultrasonography[190]. The acronym MOLES (mushroom shapre, orange pigment, large size, enlargeing tumour and subretinal fluid) can be used to help distinguish key clinical features between choroidal melanonoma and naevi (devised by B.E.D.).

Punctuated evolution
Rapid bursts of events that drive tumour fitness.

pathway and a BSE event — standing for *BAP1*, splice and *EIF1AX* mutations[76]. The actual order of oncogenic events that lead to the development of UM is starting to be elucidated. A mutation in a *GNA* family gene is suspected to be the initiating event, as these mutations are present in benign blue naevi and uveal naevi; however, the exact mechanism of progression from benign naevus to UM has yet to be analysed[15–17]. Furthermore, sophisticated recent genomic analyses support an alternative model of punctuated evolution, with almost simultaneous emergence of all oncogenic events[76].

Gα$_q$ pathway alterations. Virtually all UMs carry a mutually-exclusive hotspot mutation that activates the Gα$_q$ pathway. Mutations usually involve *GNAQ* and *GNA11*, but sporadically occur in *CYSLTR2* and *PLCB4*. *GNAQ* and *GNA11* encode α subunits (α$_q$ family) of the heterotrimeric G proteins, which normally only activate intracellular signalling pathways in response to activation; for example, CYSLTR2 is activated by leukotrienes. Most choroidal naevi carry a mutation in *GNAQ* or *GNA11* (REF.[15]), as do ~85% of UMs, most often at codon Q209; in ~5% of UMs, the mutations are at codon R183 and, exceptionally, at G48 (REFS[16,17]). L129 *CYSLTR2* and D630 *PLCB4* mutations are found in ~10% of UMs (REFS[77,78]). CYSLTR2 is a cell-surface leukotriene receptor of the G protein-coupled receptor family, which depends on Gα$_q$ for downstream signalling. L129 *CYSLTR2* and D630 *PLCB4* mutations define a signal transduction pathway that leads to the activation of protein kinases C (PKCs). The actionable small G protein ARF6 acts just downstream of Gα$_q$ and activates multiple pathways, including mitogen-activated protein kinase (MAPK), β-catenin, RhoA–Rac and Yes-associated protein (YAP)[79] (FIG. 3). Although mutations leading to activation of the Gα$_q$ pathway are present in almost all UMs, the respective roles of these pathways in oncogenesis are unclear. Several reports strongly support a major role for YAP activation in UM[80,81], with Gα$_q$ activating focal adhesion kinase (FAK) via the TRIO–RhoA pathway, and with FAK subsequently activating YAP via Mps one binder 1 (MOB1) (REF.[82]). With regard to metastases, interfering with this pathway is considered an option for treatment; Gα$_q$ mutations activate the MAPK pathway[16,17], but the relative inefficacy of MAPK inhibitors in clinical trials in patients with UM suggests an accessory role of this pathway in tumorigenesis. Drugs that directly inhibit Gα$_q$, such as FR900359 and YM-254890, do not distinguish between wild-type and mutated Gα$_q$, making them toxic and unsuitable[83,84].

BSE event. As the annual rate of malignant transformation of choroidal naevi to melanoma is estimated to be 1 in 8,845 (REF.[85]), another genetic aberration is considered essential for developing malignant potential. This subsequent BSE event consists of a biallelic inactivation of *BAP1*, a change-of-function heterozygous mutation of a splicing gene (mainly of *SF3B1*) or an N-terminal tail mutation in *EIF1AX*. *BAP1* biallelic inactivation occurs in ~50% of primary UMs, combining loss of heterozygosity (mostly monosomy 3) and a deleterious somatic mutation of the second *BAP1* allele in a two-hit model. *BAP1*-inactivated UMs are at high risk of metastatic relapse[23]. BAP1 is a nuclear deubiquitinating hydrolase with many functions[86], including protein deubiquitination, cell cycle regulation and cell growth, DNA damage repair, regulation of apoptosis[87], chromatin remodelling and regulation of gene expression. Loss of BAP1 is associated with changes in DNA methylation patterns[18,88]. Supporting its role in chromatin remodelling, the BAP1 orthologue in *Drosophila*, Calypso, was

Table 1 | **Molecular uveal melanoma subsets**

Subset	Metastatic potential	mRNA GEP	Chromosome 3	Chromosome 8q	Chromosome 6p	Key mutation	Inflammation
A	Low	Class 1	Two copies	Two copies	Partial or total gain	*EIF1AX*	No
B	Intermediate	Class 1	Two copies	Partial gain	Gain	*SF3B1*	No
C	High	Class 2	One copy	Three or more copies	No change	*BAP1*	No
D	High	Class 2	One copy	Three or more copies; isochromosome 8q	No change	*BAP1*	Yes

GEP, gene expression profile. Based on data from REFS[5,18–20].

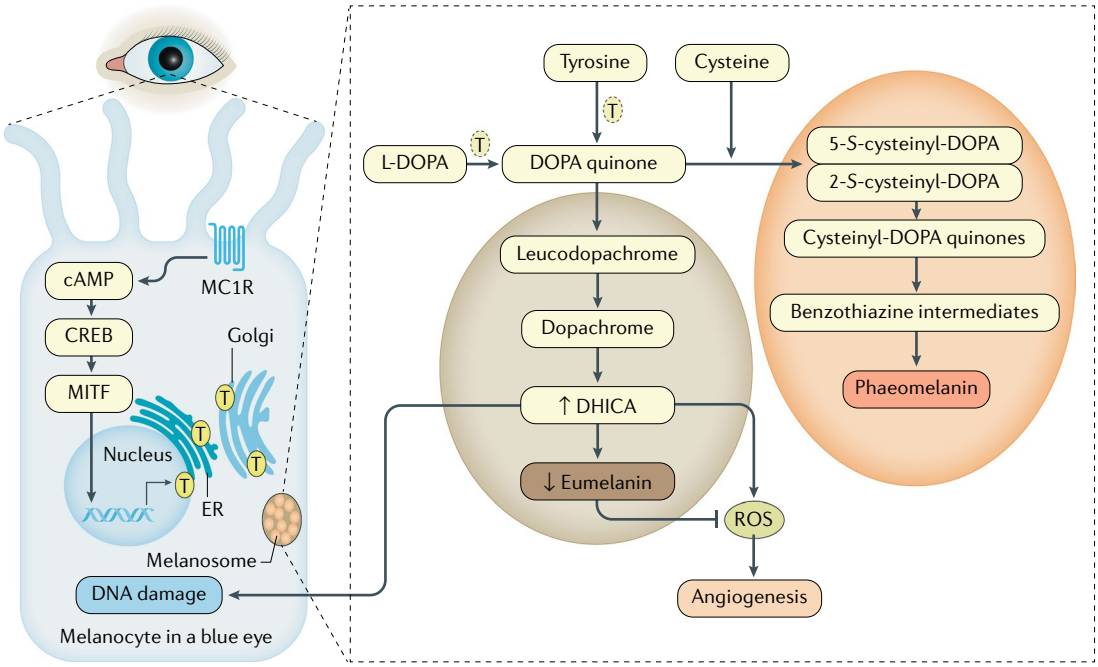

Fig. 2 | **Low eumelanin-to-phaeomelanin ratio in a blue eye.** Pale skin, red hair, freckles and an inability to tan are related to inactivating polymorphisms in the gene encoding melanocortin 1 receptor (MC1R), which results in relatively high levels of phaeomelanin (yellow–brown pigment) and the red hair and fair skin phenotype. Additionally, in melanocytes lacking functional OCA2 (which is required for normal melanin production), tyrosinase (T) — a copper-containing enzyme that catalyses the production of melanin from tyrosine by oxidation — does not traffic properly and is retained in the endoplasmic reticulum (ER)–Golgi compartments[72,73]. This accumulation leads to defective eumelanin (black–brown pigment) synthesis, but does not affect the synthesis of phaeomelanin[366]. In particular, 5,6-dihydroxy-indole-2-carboxylic acid (DHICA) accumulates, which causes single-strand breaks in plasmid DNA (following ultraviolet (UV) exposure as well as in the absence of UV)[367]. Accordingly, a low eumelanin-to-phaeomelanin ratio and high concentration of reactive oxygen species (ROS) may be a risk factor for the acquisition of somatic mutations in ocular melanocytes[71]. *OCA2* pink-eyed allele was found to be a modifier of angiogenesis in a mouse linkage scan[368]. *OCA2*-deficient mice have increased plasma levels of melanin precursors[369].

shown to form a complex with ASXL isoforms, which are epigenetic scaffolding proteins that assemble epigenetic regulators and transcription factors to specific loci with histone modifications, and shown to be part of the Polycomb machinery, which has a role in the maintenance of cell identity via transcriptional repression[89]. The Calypso–ASXL and BAP1–ASXL complexes demonstrated deubiquitinase activity towards histone H2A lysine 119 mono-ubiquitylation (H2AK119ub)[89]. Notably, one of the two main Polycomb repressive complexes (PRC), PRC1, has precisely the opposite role of the BAP1–ASXL complex, that is, it has ubiquitylase activity towards H2AK119. Indeed, recent studies have revealed that BAP1 co-localizes with RNA polymerase II and protects transcribed genes against PRC1-mediated pressure for gene silencing[90,91]. If confirmed, BAP1 would favour transcription and would negatively regulate the Polycomb machinery rather than being part of this repressor complex.

Another BSE event is a hotspot mutation in a splicing gene, most often *SF3B1*. Mutations at R625, K666 and K700 of *SF3B1* have been reported in ~25% of UMs[7,21,92]. Interestingly, mutations in R625, and less frequently in K666, prevail in UM, whereas K700 mutations are more frequent in haematopoietic malignancies. Alternatively, other splicing genes may also be involved in UM: *SRSF2* with in-frame deletions has been reported in the TCGA cohort[18]. *SF3B1* encodes a core component of the U2 snRNP complex of the spliceosome that recognizes a branch point upstream of the 3′ splice site, which is mandatory for recognition and correct splicing. *SF3B1* mutations result in the recognition of alternative branch points, thereby disrupting normal splicing of ~1% of splicing junctions. These aberrations mainly result in the usage of alternative cryptic 3′ splice sites, leading to the retention of short intronic sequences in the mature transcript[93,94]. The possible consequences of these splicing aberrations are frameshift insertions with mRNA degradation[93], but the intronic insertions are in-frame in one-third of the abnormal transcripts, potentially leading to activated or change-of-function proteins. The link between splicing aberrations, gene down-regulation or modification and malignant transformation in UM has not yet been fully clarified. Recently, *BRD9*, which encodes a core component of the non-canonical BAF chromatin-remodelling complex, was shown to be abnormally spliced and repressed, and to have a major tumour suppressor role in *SF3B1*-mutated UMs[95].

Finally, the BSE event can include mutation in *EIF1AX*. eIF1A is a component of the 43S pre-initiation complex that mediates recruitment of the small

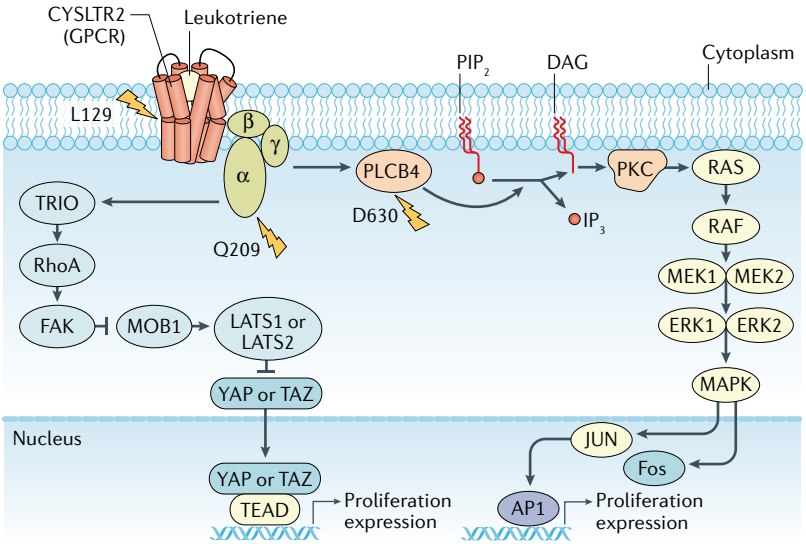

Fig. 3 | **Gα$_q$ pathway alterations.** Virtually all uveal melanomas (UMs) harbour a mutually exclusive hotspot mutation (at Q209) that activates the Gα$_q$ pathway. Activating mutations usually involve *GNAQ* and *GNA11*, but sporadically occur in *CYSLTR2* (which encodes a cell-surface G protein-coupled receptor (GPCR) for leukotrienes; at L129) or *PLCB4* (at D630). These mutations activate the YAP (or TAZ) pathway, stimulating cell proliferation, which is considered to be the main oncogenic pathway in UM. These mutations also activate the protein kinase C (PKC), MAPK and AP1 pathways, similarly activating proliferation. Based on data from REFS[82,370].

ribosomal subunit to the 5′ cap of mRNAs to initiate protein translation. Missense and nucleotide deletion variants alter the first 15 N-terminal tail codons of *EIF1AX* in ~15% of UMs[21]. *EIF1AX* mutations are thought to alter the translation initiation site and the expression of protein products but the nature of their downstream targets is yet to be defined[21,96]. It should be noted that UMs carrying an *EIF1AX* mutation are generally characterized by an excellent outcome.

Metastasis

In a study of >8,000 patients with UM, the 10-year rates for metastasis were 33% for ciliary body melanoma, 25% for choroidal melanoma[97] and 7% for iris melanoma, with deaths typically occurring 1–3 years after treatment[98] and probably associated with mutations in either *BAP1* or *SF3B1* (REFS[99,100]). The larger the primary UM, the higher the number of mutant cells generated, which includes those with *BAP1* and *SF3B1* mutations[101]. Indeed, loss of BAP1 expression can be used to differentiate between tumours with an overall 'good' or 'bad' phenotype; loss of chromosome 3 (REFS[18,102–104]) and loss of function of *BAP1* on the other chromosome 3 (REFS[18,102–104]) are usually associated with an mRNA class 2 gene expression pattern[20,23] (TABLE 1).

Two major studies analysed the genetic and genomic evolution between primary and metastatic UMs. No new driver mutations in the metastasis and very few new mutations were associated with tumour progression, and limited heterogeneity was observed at this level. Most importantly, BAP1 was not inactivated during tumour progression of *BAP1* wild-type UMs, indicating that *BAP1* inactivation is an early event in tumorigenesis and not acquired during metastatic progression. Furthermore, additional recurrent copy number changes (losses of 1p, 6q and 8p; gains of 1q, 6p and 8q; and isodisomy 3) were associated with tumour progression. Finally, mutations of chromatin-remodelling factors, such as *PBRM1* and *EZH2*, seem to occur as late events in tumour evolution[105,106]. These results support a sequence of events in UM that begin with *BAP1* and involve *PBRM1*, *EZH2* and — probably — other genes at later stages[107].

The liver is the most common site of metastases, but metastases can occur in other organs, such as the lungs, lymph nodes, bone, skin and brain. The metastatic process in UM can be divided into three compartments: the primary tumour, haematopoietic tissue and liver. UM intravasation into blood vessels occurs in the primary tumour; tumour cells enter the systemic circulation, where they pass through the right side of the heart, the lungs, the left side of the heart and the aorta before being introduced from the systemic circulation into haematopoietic tissue, including bone marrow and the spleen[108,109]. Experimental evidence shows that UM cells and bone marrow-derived cells (BMDCs) exit the bone marrow, pass through the heart and lungs, and are introduced into the spleen and liver[110]. Direct evidence from human specimens shows that cMET expression by UM cells plays a part in their affinity for the liver[111], as the ligand of cMET, hepatocyte growth factor (HGF), is produced by hepatic stellate cells[112]; the cMET–HGF axis involvement has been shown in a mouse model of metastatic UM[113]. Homing to the liver also involves UM expression of CXCR4[114,115]; its ligand CXCR12 (also known as stromal cell-derived factor (SDF1)) is produced by hepatic sinusoidal endothelial cells and hepatic stellate cells[115,116]. Blocking the CXCR4–CXCR12 axis or the cMET–HGF axis blocks the development of metastases in mice[117,118]. In the liver, there is direct evidence from human specimens[119] and evidence from a mouse model[120] that individual UM cells can infiltrate the parenchyma or exhibit periportal localization and eventually exhibit angiogenesis, which is essential for tumours to grow in this metastatic location.

Metastatic UM may be present in the sinusoidal spaces in the liver in an infiltrating growth pattern and in the periportal areas in a nodular growth pattern (FIG. 4)[119]. Both growth patterns may be present in the same liver and the nodular pattern may give rise to the infiltrating pattern in some instances[121]. The infiltrating growth pattern of UM is dependent on the creation of pseudosinusoidal spaces by hepatic stellate cells, whereas the nodular growth pattern is dependent on angiogenesis in the periportal areas[119,122]. Metastatic growth is promoted by hypoxia-induced collagen production by hepatic stellate cells in the infiltrating pattern and hypoxia-induced production of vascular endothelial growth factor (VEGF) by melanoma cells in the nodular growth pattern[119,123]. VEGF is counterbalanced by hepatic stellate cell production of pigment epithelium-derived factor (PEDF), whereas the melanoma cells themselves produce platelet-derived growth factor and transforming growth factor-β, which blocks PEDF production by the hepatic stellate cells[124]. Thus, we (H.E.G.) hypothesize that there is a balance of PEDF and VEGF in the liver,

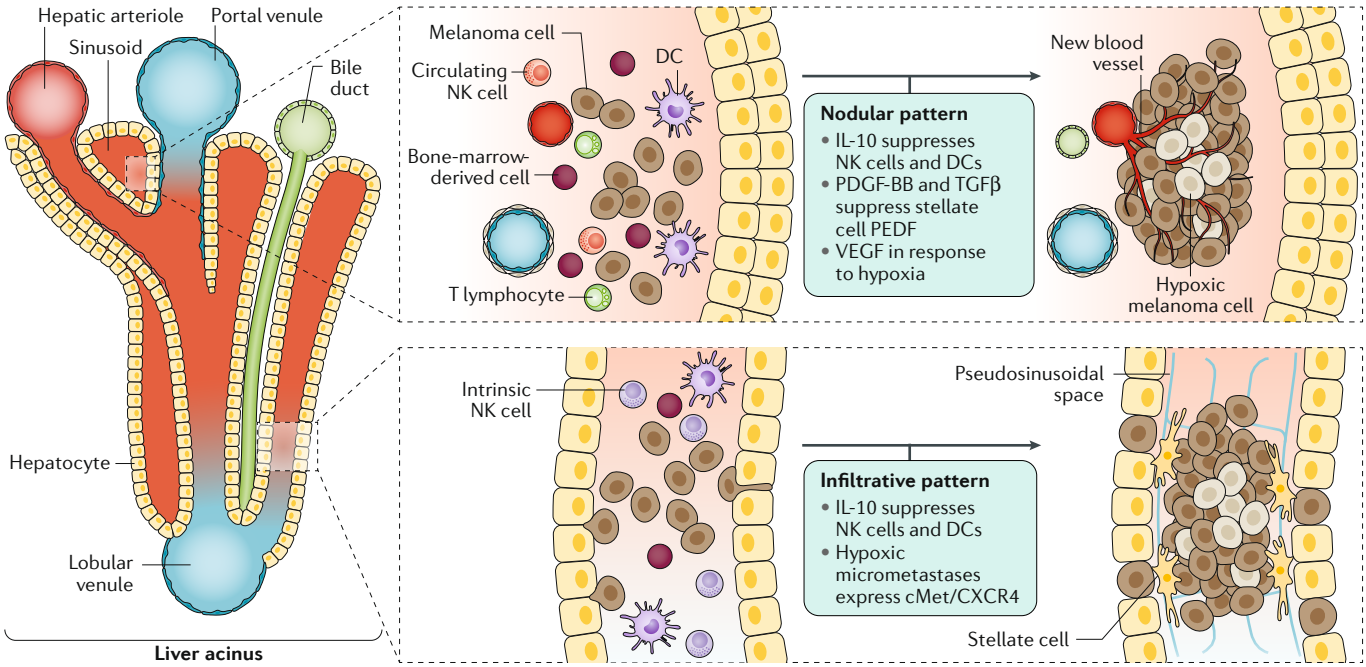

Fig. 4 | **Metastatic UM in the liver.** Metastatic uveal melanoma (UM) in the liver can demonstrate periportal nodular growth patterns (top) or sinusoidal infiltrative growth patterns (bottom). In the periportal nodular growth pattern, UM cells localize in the periportal areas, become hypoxic and the tumour exhibits angiogenesis with the production of vascular endothelial growth factor (VEGF). In the infiltrative pattern, the tumour lodges in the sinusoidal spaces, develops its own circulation via hepatic stellate cell-lined pseudosinusoidal spaces and exhibits some hypoxia; the cMET and CXCR4 axes are activated to promote growth. Regardless of which pattern is involved, immune factors that enable UM growth include bone marrow-derived cell-mediated IL-10 suppression of natural killer (NK) cells. Non-immune factors include UM production of platelet-derived growth factor (PDGF-BB) and transforming growth factor-β (TGFβ), which suppress hepatic stellate cell pigment epithelium-derived factor (PEDF). DC, dendritic cell. Adapted with permission from REF.[371], Elsevier.

and once this balance favours VEGF, the metastatic UM grows.

Immunology and inflammation

Although tumour-specific antigens and tumour-specific T cell responses to UM have been identified, antitumour immune responses do not seem to affect UM metastasis. Furthermore, the low responsiveness of metastatic UM to immune checkpoint inhibition suggests that the immune-privileged environment of the eye influences the induction and/or effector phase of the immune response. Other hypotheses for this unresponsiveness include: that immune cells cannot infiltrate UMs; that UM cells are not immunogenic, cannot be recognized by immune cells and are resistant to immune attack; and that UM cells induce immune tolerance.

Immune privilege. Animal studies (BOX 3) have shown that the intraocular environment promotes tumour growth, and several lines of evidence support the notion that the eye has immune privilege, with an intraocular environment that derails normal immune reactions. For example, highly immunogenic, syngeneic tumours that are routinely rejected when placed extra-ocularly survive and grow when placed in the eye[125,126], a characteristic known as anterior chamber-derived immune deviation (ACAID). Tumour cells placed in the anterior chamber of the eye in mice actively downregulate cellular immune reactions in delayed-type hypersensitivity (DTH)[127,128]. Furthermore, the subretinal space and vitreous cavity similarly function as immunologically privileged sites[129]. Although DTH responses are downregulated, intraocular tumours have been shown to induce cytotoxic T cells (CTLs) in mice and to be susceptible to CTL-mediated lysis[130].

Leukocyte infiltration. UMs have the lowest leukocyte fraction of all cancer types studied by the TCGA[131]. However, although many UMs lack an infiltrate, a minority of tumours have considerable immune infiltration, namely type D tumours[22,132] (TABLE 1). UMs with a moderate or intense immune infiltrate are larger and have more vascularization[133]. UM-infiltrating leukocytes have been shown to be mainly T cells and macrophages, with hardly any B cells or natural killer (NK) cells[134]. The majority of tumour-infiltrating lymphocytes are $CD8^+$ T cells that are activated, as shown by expression of HLA-DR[134]. Tumour infiltrates also contain $FOXP3^+$ regulatory T cells[135,136]. The presence of macrophages seems to be associated with tumours showing gain of chromosome 8q; T cell infiltrate seems to be associated with tumours showing monosomy 3 and loss of *BAP1* (REFS[135,137]). These findings indicate an association between genetic tumour evolution and the development of an inflammatory infiltrate. Using the TCGA data, *BAP1* loss was associated with an upregulated expression of several genes that are

Box 3 | **Animal models of UM**

In vitro and in vivo models of uveal melanoma (UM) are being used to understand the effects of the immunologically privileged eye on tumour growth and to develop and screen new treatments. The development of xenograft models has improved the efficiency of drug screening and may provide models for personalized tumour targeting[343]. Prior to xenograft model use, inoculation of murine or human UM cell lines into immunodeficient or immunosuppressed animals was used[344] (namely, rats[345], rabbits[346] or zebrafish[347]). Unfortunately, the complex molecular landscape of UM can barely be reflected using cell lines[348], as most lack monosomy 3 or loss of BAP1 (REF.[349]). Instead, individual patient-derived xenograft (PDX) models, which may phenotypically and genetically exhibit the characteristics of the primary and metastatic tumours, have been developed[350] to help determine the most effective therapy for individual patients[351]. However, the necessary immunodeficiency in the animals is a major problem.

More recently, transgenic animal models of UM have become available. The first transgenic mouse model was induced by expression of oncogenic *GNAQ*^{Q209L} under the control of the Rosa26 promoter and shows neoplastic proliferation in the choroid, along with dermal naevi and other melanocytic neoplasms, with 94% of mice subsequently developing lung metastases[352]. Combining mutant *Tp53* with *GNAQ*^{Q209L} or *GNA11*^{Q209L} transgenesis led to the development of melanocytic tumours, including UM, with near complete penetrance[353]. Mouse models with melanocyte-specific expression of *GNA11*^{Q209L} with or without homozygous *BAP1* loss have also been generated; the models develop pigmented neoplastic lesions from melanocytes of the skin, eye, leptomeninges, lymph nodes and lungs[354].

A feasible animal model of UM with liver metastases has not yet been established. However, using cell lines derived from a confirmed metastatic origin and injecting them into the liver or spleen leads to multiple hepatic and intra-abdominal metastases, mimicking those observed in human hepatic metastases of UM[355,356].

associated with immunosuppression, such as CD38 and CD74 (REF.[138]). These data indicate that although tumours may contain a leukocytic infiltrate, the inflammation is immunosuppressive in nature.

Immunogenicity. A lack of neoantigens expressed by UMs may underlie the inefficacy of immune checkpoint inhibitors[139,140]. These neoantigens provide a stimulus and target for new immune responses. As UMs harbour few mutations, they are not expected to express neoantigens. However, UMs express many pigment-related antigens that can be recognized by T cells, such as tyrosinase, tyrosinase-related protein 1 (TRP1), melanoma antigen recognized by T cells 1 (MART1) and the melanocyte protein PMEL, also known as gp100 (NKI-beteb)[141,142]. The melanoma antigen gene (MAGE) antigens, which are usually expressed on male germ cells, and often on cancer cells, are not expressed by UM or its metastases[143]. However, in one study, preferentially expressed antigen in melanoma (PRAME) was found to be expressed on UM and on its metastases, and may be an interesting target[144,145].

In many malignancies, tumour cells escape from T cell-mediated immune responses by losing expression of one or more *HLA* alleles[146]; loss of allele-specific HLA expression occurs in UM[147], and may play a part in the lack of immune recognition. However, unexpectedly, in UM, an inverse correlation between HLA class I expression and survival has been observed, with low HLA class I expression being associated with good survival[18,148–151]. This correlation is thought to be mediated via NK cells; a mouse model of cutaneous melanoma lacking HLA class I expression had an increased number of metastases when NK cells were depleted[152]. That is, NK cells eliminate tumour cells with a low HLA class I expression[153] and prevent tumour infiltration into the hepatic lobule[120], providing an explanation for UMs with low HLA class I expression developing fewer liver metastases[151].

A high HLA expression is part of an inflammatory phenotype: tumours that have a high HLA class I expression have high numbers of infiltrating T cells and macrophages[22,154]. This infiltrate leads to the production of pro-inflammatory cytokines such as IFNγ, and gives rise to upregulation of HLA class I and II antigen expression on UM cells[155,156]. Tumour-infiltrating macrophages tend to be of the M2 (pro-angiogenic) type; in UM, a high density of macrophages is correlated with a high mean vascular density, large tumour diameter, involvement of the ciliary body and monosomy 3 (REFS[157–159]). Influx of macrophages is also associated with an early genetic change in UM (namely, addition of extra copies of chromosome 8q), whereas the subsequent loss of one chromosome 3 and loss of *BAP1* expression is associated with a further influx of macrophages and an influx of T cells[137], and with an increased microvascular density[160]. This finding implies that loss of the BAP1 protein may regulate local inflammation in multiple ways: not only by being associated with an immunosuppressive environment, as discussed below, but also through the stimulation of an influx of macrophages and the development of blood vessels, which are necessary for systemic spreading. However, patients with UM who have increased percentages of $CD11b^{+}CD15^{+}$ myeloid-derived suppressor cells (MDSCs) in their peripheral blood have an associated impaired T cell function[161]. The role of BMDCs and MDSCs in metastatic UM is under investigation.

Immune evasion. Upon presentation of an antigen in the context of the appropriate HLA molecule, co-stimulatory molecules, such as CD80 and CD86, which bind to CD28 on the T cell, are needed to trigger an immune response. UM cells lack these co-stimulatory molecules[162]. Genetic modifications to introduce these molecules into UM cell lines have resulted in enhanced anti-UM T cell responses in vitro[163].

UM cells can inhibit the proliferation of T cells in a so-called mixed lymphocyte reaction[164] through the expression of specific ligands — that is, immune checkpoints — that bind to T cell receptors. The immune checkpoint blockade genes expressed in UM include CTLA4, PD1, PDL1, TIGIT and LAG3 (REFS[18,165–167]). An essential characteristic of UM cells is that their resistance to CTL-mediated lysis increases in the presence of IFNγ[168]. As T lymphocytes produce this cytokine, the UM cells present a very strong defence against these CTLs[168]. This phenomenon is probably caused by the upregulation of the different immune checkpoint molecules, as was shown for PDL1.

Additionally, UM cells may produce immunosuppressive cytokines, such as IDO1, that have the same function[169].

Systemic immune responses. The majority (72%) of patients with UM have developed antitumour antibodies at a higher rate than patients with carcinoma metastases in the uvea (26%) or healthy controls (13%), indicating that the tumour cells are able to induce a systemic

Neoantigen
Antigens arising from expressed mutations in tumour cells.

Fundus
The back of the eye.

immune response[170]. Furthermore, the anti-UM antibodies are complement-fixing, indicating that they might be able to kill UM cells[171]. However, the presence of these antibodies does not prevent tumour growth or metastasis formation; this may be due to the expression of membrane-bound regulators of complement activation on UM cells[172].

The majority of patients with UM harbour peripheral blood lymphocytes that are able to lyse UM cells in vitro[173], suggesting that the activity of CTLs is intact. Recovered tumour-infiltrating lymphocytes that were expanded in vitro had the capacity to react nonspecifically with HLA-mismatched UM cells[174,175], indicating a broad reactivity. Similarly, tumour-infiltrating lymphocytes could be recovered from UM metastases[176], again suggesting that UM are immunogenic and that patients are able to raise anti-UM T cell responses. Interestingly, metastases that were heavily pigmented inhibited the outgrowth of tumour-infiltrating lymphocytes[176], suggesting that tumour characteristics have a role in dictating the immune response — a feature that needs further investigation.

Further proof of activity of UM tumour-infiltrating lymphocytes comes from the treatment of patients with progressive metastatic disease with autologous, metastasis-derived tumour-infiltrating lymphocytes. After metastasectomy to grow these cells ex vivo, patients were treated with lymphodepletion and IL-2 and then reinfused with the expanded cells. Of the 20 evaluable patients, seven showed objective tumour regression, but all had severe adverse effects and one died of sepsis[177]. These data all indicate that patients with UM are able to raise an immune response against their tumours.

Tolerance and resistance. Although UM can metastasize to the bone marrow[108], this paradoxically may have a positive prognostic effect[109]. Once the bone marrow is exposed to UM cells, we (H.E.G.) propose that there is an ensuing immunological balance between CTLs that are primed by the UM[178] and NK cells, which suppress IL-10-secreting BMDCs[110]. Animal models show that once the balance shifts towards less NK activity, dormant micrometastases, particularly in the liver, have the capacity to grow[152]. Senescence of the immune system, as occurs with ageing[179], may also be a factor in the emergence from dormancy of UM cells, although this has not been analysed in UM.

We can conclude that although UMs induce systemic immune responses and UM cells can be lysed by tumour-infiltrating lymphocytes, the induced immune cells are not effective enough to overcome the immunosuppressive environment that they encounter in a metastasis, or that they cannot penetrate the metastases. As a combination of mechanisms prevents the effectiveness of the anti-UM immune responses, combining treatments may be a way forward.

Diagnosis, screening and prevention

Visual symptoms of choroidal and ciliary body tumours that should lead to a referral include blurred or distorted vision, visual field loss or photopsia[11]; patients are usually referred to an ocular oncologist through an optometrist, family doctor or ophthalmologist. However, a study from the Liverpool Ocular Oncology Centre, UK, between 1996 and 2011, showed that of 2,384 patients diagnosed with UM, one-third of patients with UM were asymptomatic[11]. Due to the rarity of the disease, no population screening takes place. As risk factors are mainly genetic, and a role for UV radiation is ambiguous, no specific advice can be given regarding preventive measures. Whether wearing sunglasses helps to reduce the risk of UM is unknown.

In terms of public health innovations in diagnosis and treatment of choroidal melanoma, in the UK, a nurse-led ocular oncology clinic proved to be feasible[180]. In Brazil, the use of WhatsApp-based telemedicine and YouTube videos to help local ophthalmologists to establish the diagnosis and to treat the patients locally without the need for travel have been reported[181] (Oculonco). The ophthalmologist examines the eye fully, including the fundus (FIG. 5), and the diagnosis of UM is achieved by recognizing classic tumour features, using eye slit lamp biomicroscopy and indirect ophthalmoscopy, combined with the results of a wide range of diagnostic tests[182–189]. Several different imaging modalities are critical to differentiate between benign naevi and malignant melanoma[190], and between melanoma and other tumours.

Imaging

Several techniques are available to diagnose UM. Slit lamp biomicroscopy and indirect ophthalmoscopy are primary imaging modalities, but gonioscopy and transillumination may be applied as well. A general ophthalmologist may deploy fluorescein angiography in the differential diagnosis of a fundus lesion, and then refer a patient with a suspicious lesion to a specialized ocular oncology centre. An ophthalmic oncologist will use ultrasonography and anterior segment ultrasonography, and will apply sophisticated techniques such as optical coherence tomography (OCT). Whichever technique is used, limitations need to be taken into consideration, as many of these techniques rely on visual identification of tumour characteristics.

Slit lamp biomicroscopy and indirect ophthalmoscopy. All patients undergo evaluation of the anterior segment of the eye with slit lamp biomicroscopy and of the posterior segment with indirect ophthalmoscopy (FIG. 5) to determine tumour location, configuration, pigmentation, vascularity, discreteness of margins, distances from the foveola and optic disc, involvement of ciliary body and angle, and anteriorly located extrascleral extension. These methods also identify secondary features such as episcleral sentinel vessels, cataract, subretinal fluid or orange pigment on the tumour. Several features have been identified as risk factors for choroidal naevus transformation into melanoma[190]. To highlight five key clinical features distinguishing choroidal melanomas from naevi (moles), we (B.E.D.) devised the acronym MOLES, which stands for mushroom shape, orange pigment, large size, enlarging tumour and subretinal fluid.

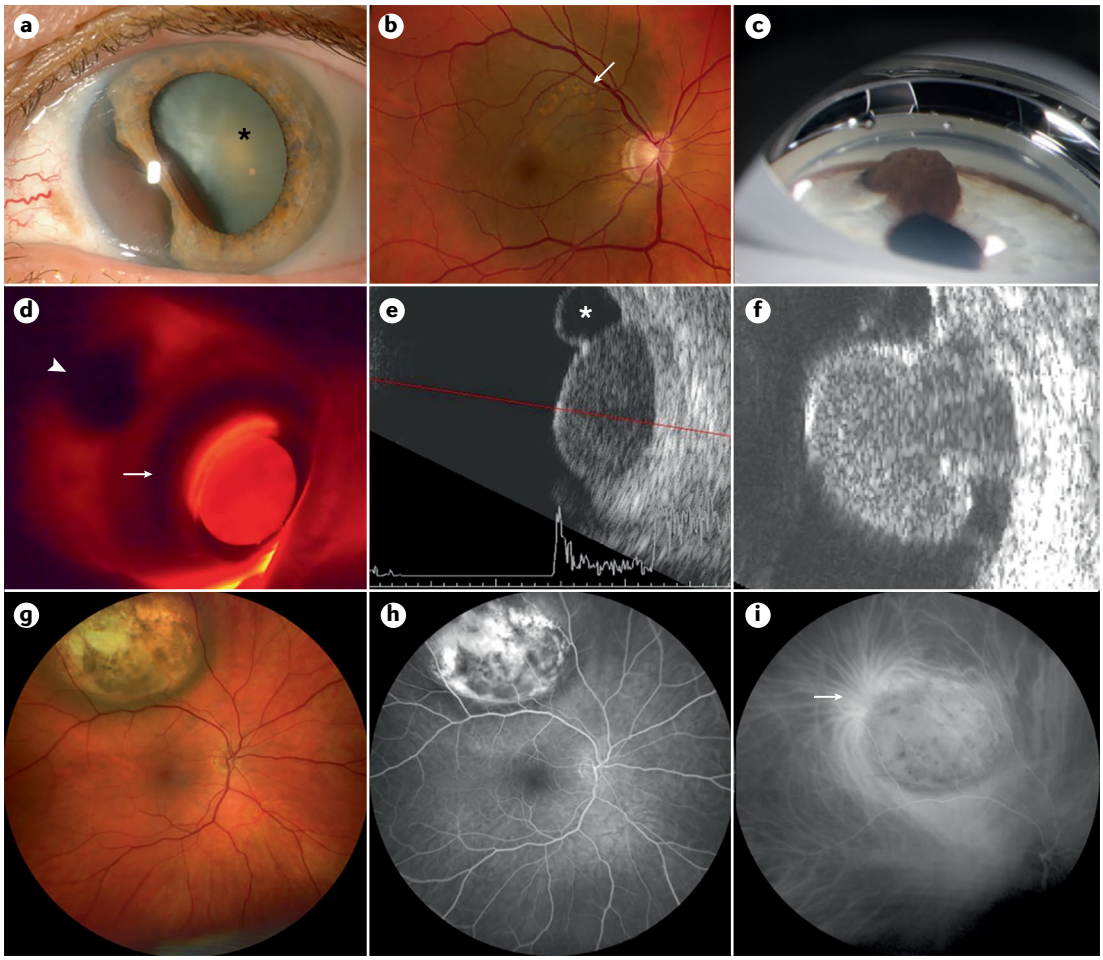

Fig. 5 | **Imaging techniques in uveal melanoma. a** | Iris melanoma with ciliary body invasion, cataract (asterisk) and lens subluxation (not visible) as examined by slit lamp biomicroscopy. Note the prominent episcleral vessels medially, the so-called sentinel vessels, signifying a ciliary body tumour. **b** | Thin choroidal melanoma located adjacent to the optic disc, with overlying orange pigment (arrow), as examined by indirect ophthalmoscopy. **c** | Gonioscopic photograph showing a pigmented iris tumour (probably a melanoma), with pigment in the anterior chamber angle. **d** | With transillumination, a bright fibre-optic light is placed on the conjunctiva or cornea, opposite the meridian of the suspected melanoma, which casts a shadow on the sclera thereby allowing the tumour extent to be defined (arrowhead). The ciliary body is visible as a dark ring (arrow). **e** | B-scan ultrasound image of a dome-shaped choroidal melanoma, which shows low internal acoustic reflectivity, demonstrated by the A-scan shown at the lower edge of the image (the red line shows the section of the A-scan). There is a bullous retinal detachment adjacent to the tumour (asterisk). **f** | B-scan ultrasound image of a mushroom-shaped choroidal melanoma. The apical part of the tumour has grown through the Bruch's membrane, which has compressed the tumour veins to cause oedema and swelling. **g** | Fundus photograph of a dome-shaped, choroidal melanoma, which is amelanotic and, therefore, needs to be differentiated from metastasis by systemic investigations and/or tumour biopsy. **h** | Fluorescein angiogram of the melanoma displayed in panel **g**, showing the amelanotic tumour as diffusely hyperfluorescent with areas of hypofluorescence owing to 'masking' by remnants of the retinal pigment epithelium. **i** | On the indocyanine green angiogram, the tumour is diffusely hyperfluorescent. The choroidal blood vessels are also clearly displayed (arrow).

Gonioscopy and transillumination. Gonioscopy (a technique to evaluate the periphery of the anterior segment of the eye; FIG. 5) can establish the presence and degree of anterior chamber angle invasion of an iris or ciliary body melanoma, which extends anteriorly[186]. This technique is performed using a gonioscopic lens with tilted mirrors that reveal details in the opposite angle. Melanoma with invasion of the angle is associated with a higher risk of glaucoma and metastatic disease.

Transillumination (in which a bright light is shone into the eye to determine the extent of ciliary body involvement; FIG. 5) can be achieved by transcleral or transpupillary illumination. A bright fibre-optic light in the conjunctival fornix, opposite the meridian of the melanoma, casts a measurable shadow through the sclera that denotes the tumour extent. Cystic lesions and some tumours, such as leiomyoma, do not cast a shadow.

Ultrasonography and ultrasound biomicroscopy. Ultrasonography is the most-used application to determine the dimensions of a posterior UM. Ultrasonography is also essential throughout follow-up, to measure the tumour. There are two types of ocular ultrasonography: A-scan for internal reflectivity and B-scan for echodensity qualities. With A-scan ultrasonography,

Glaucoma
A group of eye disorders characterized by damage to the optic nerve.

Lipofuscin
An insoluble yellow-brown to dark brown pigment derived from incomplete oxidation of lipids.

a UM shows medium to low internal reflectivity, demonstrating a high peak on the tumour apex, then a gradual decrease in reflectivity as the sound wave travels through the mass. With B-scan ultrasonography (FIG. 5), a UM shows a dome, mushroom or flat surface configuration[191]. Additional features of a B-scan include acoustic hollowness and choroidal excavation. In a few patients, ultrasonography can disclose orbital extension of the tumour where the tumour grows through the sclera, usually via an emissary canal. The presence of intrinsic vascular pulsations on B-scan is strongly suggestive of a solid tumour rather than haemorrhage. In eyes with opaque media from cataract or vitreous haemorrhage, the tumour cannot be visualized; instead, the ultrasound waves can be transmitted through the opacification to image the posterior segment of the eye[191]. In some instances, ultrasonography might reveal one or more cavities within the mass, suggestive of cavitary UM[192].

Ultrasound biomicroscopy is a variation of ultrasonography that is used to image and measure iris and ciliary body tumours[193,194]. This is particularly important to determine the extent of a ciliary body mass, any spread through the scleral wall and to determine if an iris tumour has invaded the ciliary body.

Angiography and autofluorescence. Fluorescein angiography is a technique whereby fluorescein dye is injected intravenously to image the retinal and choroidal vasculature and retinal pigment epithelial abnormalities (FIG. 5). On fluorescein angiography, UMs show slow flow with mottled hyperfluorescence in the vascular filling phases and diffuse late staining of the mass, often into overlying subretinal fluid. Much can be learned from looking at fluorescence images, identifying changes caused by the tumour versus changes in the tumour-associated retinal pigment epithelium[195,196]. Smaller UMs remain hypofluorescent, whereas larger UMs, particularly those with a mushroom configuration, can show prominent intrinsic vascularity in a haphazard pattern termed double circulation, showing retinal and tumour vessels. Areas of UM invasion into the overlying sensory retina are hypofluorescent with staining at the margins. Fluorescein angiography can also document preretinal or subretinal neovascularization, which is particularly important as preretinal neovascularization can result following ischaemia induced by radiotherapy. Indocyanine green angiography is a technique whereby indocyanine dye is injected intravenously to image the choroidal vessels (FIG. 5). Small UMs are hypocyanescent, whereas large UMs are hypercyanescent[197]. This technique is particularly valuable when visualizing the pattern of choroidal blood vessels within the tumour, especially when there is overlying blood, and also to rule out other tumours that show a different vascular pattern, such as choroidal haemangioma.

Autofluorescence photography is a non-invasive retinal imaging modality to detect lipofuscin in the retinal pigment epithelium (FIG. 6). This correlates with 'orange pigment' that can be seen by indirect ophthalmoscopy, which can be useful in the early diagnosis of small UMs that often have overlying lipofuscin and give rise to geographic hyperautofluorescence[198–200]. Choroidal naevi tend to be iso-autofluorescent or hypo-autofluorescent, whereas melanomas demonstrate hyper-autofluorescence[198,199]. After treatment, blue-light fundus autofluoresce imaging can be used to identify whether a radioactive plaque was properly located[201].

Optical coherence tomography. OCT is an imaging method based on low coherence interferometry of light to image the posterior segment of the eye. OCT reliably demonstrates subtle retinal abnormalities, such as subretinal fluid, intraretinal oedema, cystoid macular oedema and the cross-sectional configuration of a choroidal mass (FIG. 6). This technique is best employed for small UMs (<3 mm in thickness) as the depth of focus

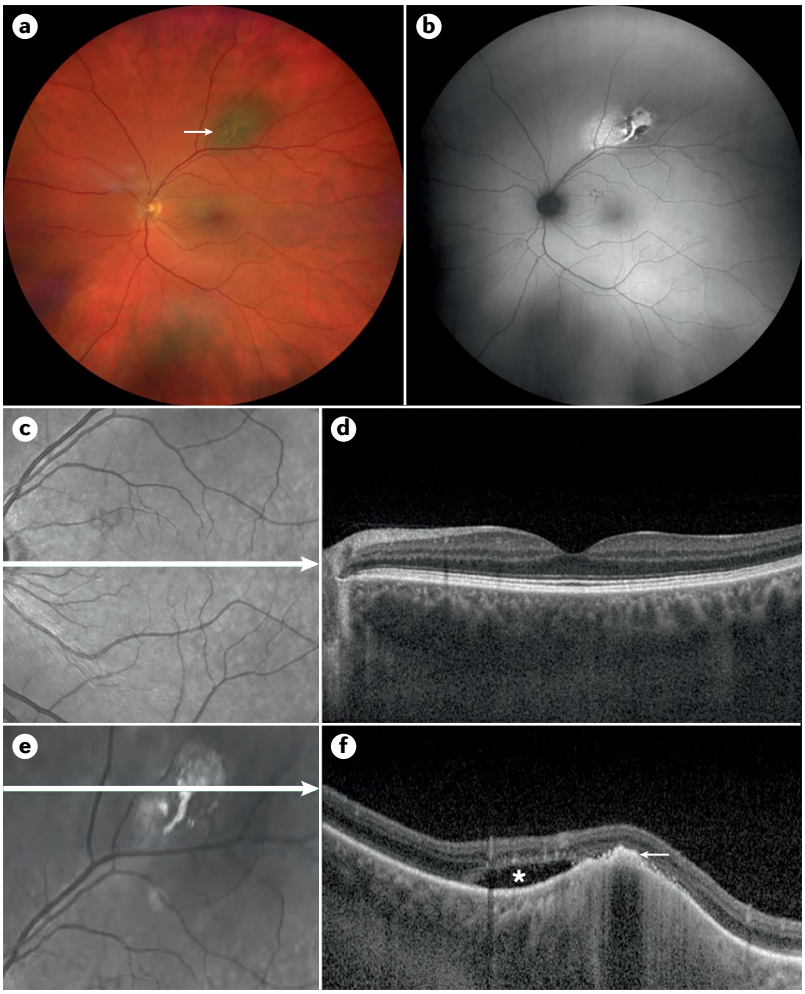

Fig. 6 | **Small choroidal melanoma with orange pigment and shallow subretinal fluid in a young man.** Thin choroidal melanoma located superior to the left macula, with overlying orange pigment (representing lipofuscin) and subtle subretinal fluid. **a** | Colour fundus photograph. The peripheral dark areas away from the tumour are part of the normal choroidal pigment distribution. **b** | The tumour in panel **a** (arrow) appears hyperautofluorescent on the autofluorescence photograph where lipofuscin has accumulated. **c**,**d** | Optical coherence tomography (OCT) image over the fovea of this eye shows no abnormalities. The arrow in panel **c** shows the location of the section shown in panel **d**. **e**,**f** | OCT image over the tumour reveals subretinal fluid (asterisk in panel **f**) and lipofuscin clumps on the tumour surface (arrow in panel **f**).

Bruch's membrane
The innermost layer of the choroid, also known as the vitreous lamina.

includes the posterior vitreous, retina, choroid and, in some patients, sclera[190,202–206]. OCT is valuable for early detection of UM, especially when considering factors for distinguishing a choroidal naevus from a UM[190,206]. By OCT, many UMs show a dome-shaped configuration, rarely with retinal invasion. The tumour compresses the choroidal vasculature, especially the choriocapillaris[205,207]. By contrast, choroidal metastasis shows a 'lumpy' or 'bumpy' surface and choroidal lymphoma shows an undulating surface. Often, UMs with overlying subretinal fluid show fresh 'shaggy' photoreceptors that probably represent macrophages in the elevated retina. For iris melanoma, OCT has been adapted to the anterior segment; however, deeply pigmented tumours tend to obstruct light transmission such that the basal tumour margin is not visible. In such cases, ultrasound biomicroscopy is more informative[194]. Additionally, OCT angiography demonstrates retinal blood flow using OCT and split-spectrum amplitude decorrelation angiography. OCT angiography is used mostly for retinal imaging and not choroidal imaging; however, studies have found that eyes with UM show remote retinal microvasculopathy with macular ischaemia[208]. The most common use of OCT angiography is to detect macular microangiopathy following radiotherapy[209], which can be treated. When looking at oximetry data, retinal vessels in the non-involved part of the eye containing a UM show an increased arteriovenous difference, indicating that a UM may influence oxygen use in the whole retina[210].

CT and MRI. CT is rarely used to visualize UM, but it is sometimes valuable for delineating large tumours or orbital invasion[211]. For most UMs, ultrasonography is sufficient for imaging, but MRI can be useful to measure the basal diameters of a ciliary body UM. MRI is more valuable than CT for imaging a UM or orbital extension, particularly with large tumours, and MRI can detect extrascleral extension of tumour[212]. MRI has high resolution and UMs show a fairly typical pattern on T1-weighted images, demonstrating a bright signal relative to the vitreous compared with T2-weighted images, which provide a low (dark) tumour signal compared with the vitreous[213] (FIG. 7). UMs show bright enhancement with gadolinium, a feature that differentiates the solid tumour from vitreous or a subretinal haemorrhage. The most valuable use of MRI in UM imaging is in eyes with opaque media.

Biopsy

Biopsy is a valuable method to establish the diagnosis of UM when clinical examination and imaging are inconclusive[214]. The most commonly employed technique is fine-needle aspiration biopsy whereby a 27-gauge needle is passed through the sclera and vitreous under guidance by indirect ophthalmoscopy. Other methods use devices such as the Essen forceps, which 'bite' a pellet-shaped specimen from the tumour, or a vitreous cutter. Biopsy is also instrumental in tissue sampling for the cytogenetic or gene expression study of UM[215–219]. Biopsy is regarded as a safe procedure when performed by an experienced ocular surgeon.

Histopathology. The gross appearance of UM in enucleated eyes includes elongated, nodular or mushroom-shaped. These tumours may be pigmented (melanotic), non-pigmented (amelanotic) or a mixture of the two (FIG. 8). If the tumour has broken through the Bruch's membrane and has a mushroom shape, the portion of the tumour that has broken through the Bruch's membrane will exhibit vascular dilation, as that portion of the tumour is considered to be 'choked off' by the Bruch's membrane, resulting in vascular congestion. Extraocular extension of UM usually occurs via vortex veins or along nerves or blood vessels in emissary canals in the sclera, especially posteriorly.

UM is composed of a mixture of cells, including tumour cells, infiltrating macrophages and lymphocytes, fibroblasts and blood vessels. The cytological classification of UM is based on microscopic analyses and follows the modified Callender classification, which characterizes UM cells[220,221]. Spindle A cells are fusiform and the nucleus contains a central fold, or groove. These cells are now considered to be naevus cells. Spindle B cells are also fusiform, contain a spindle-shaped or cigar-like nucleus with a prominent nucleolus and are the most common cell type in UM. Epithelioid cells are non-cohesive and round, and contain a large round nucleus with a large prominent eosinophilic nucleolus; this cell type is associated with poor outcome. So-called intermediate cells (small epithelioid cells) are an intermediate between spindle B and epithelioid melanoma cells. A melanoma that is composed of at least 90% spindle B cells is a spindle cell-type melanoma, and a melanoma that is composed of at least 90% epithelioid cells is an epithelioid cell-type melanoma; all other tumours are mixed cell-type melanomas, which are the most common (FIG. 9). Regardless of cell morphology, the most important immunohistochemical markers expressed by choroidal melanoma are HMB45, S100, PMEL, Melan A, MITF, tyrosinase and SOX10 (REFS[141,222–224]).

Iris melanomas (FIG. 10a,b) are characterized histologically by spindle and epithelioid cells. Many lesions classified as iris melanomas (BOX 1) in the past are likely to have been naevi, when looking at their clinical course and molecular characteristics. Ciliary body UMs may be insidious due to their location behind the iris (FIG. 10c,d). There may be sentinel vessels in the episclera overlying these tumours. Both tumour types may contain spindle and epithelioid cells.

Tumours are categorized into different tumour–node–metastasis (TNM) categories as defined by the American Joint Committee on Cancer (AJCC)[225]. The categories are related to the likelihood of developing metastases (see below).

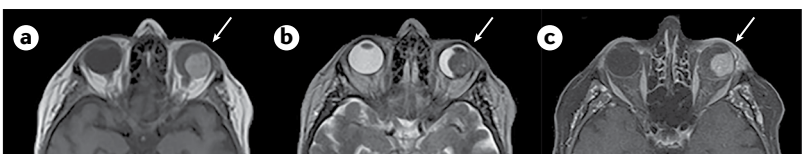

Fig. 7 | **MRI of uveal melanoma.** All images are from the same patient, with a large choroidal melanoma (arrows). T1-weighted (panel **a**), T2-weighted (panel **b**) and T1-weighted fat-suppressed (panel **c**) images with gadolinium enhancement are shown.

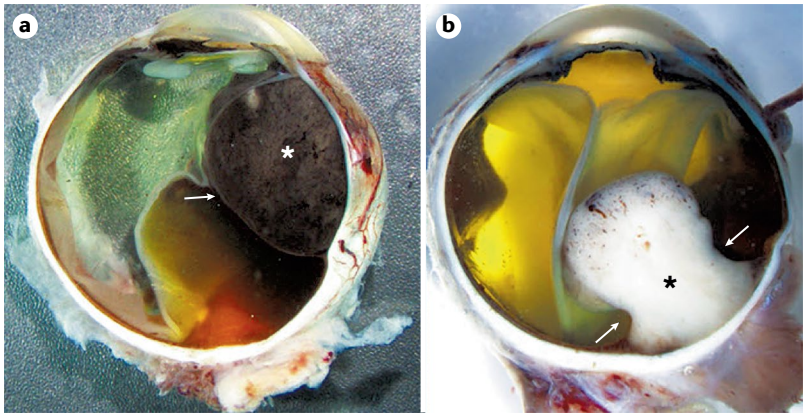

Fig. 8 | **Gross appearance of UM. a** | A heavily-pigmented uveal melanoma (UM; asterisk) confined by the Bruch's membrane (arrow). There is an adjacent retinal detachment. **b** | An amelanotic UM (asterisk) breaking through Bruch's membrane (arrows) in a mushroom-shaped configuration.

Prognosis

Over time, a wide range of histological factors have been linked to metastasis formation and prognosis, such as cell type, pigmentation, size (largest dimension), intrascleral and extrascleral extension, ciliary body involvement, mitotic activity, location of the anterior margin of the tumour and optic nerve extension[221]. The size of the melanoma is also correlated with outcome: in a study in 8,033 patients, each millimetre of increased thickness added 5% risk of metastasis at 10 years[97]. Additionally, vasculogenic mimicry (VM) patterns, whereby cancer cells generate structures that may allow flow of fluids, have been identified in UM, of which arcs with branching, closed vascular loops and vascular networks are associated with increased risk of metastasis[226]. These VM patterns include fibrovascular septae, melanoma cell-lined channels and endothelial cell-lined vessels. We can accurately predict a patient's chance of developing metastasis; however, as primary ocular treatment of the eye with a UM does not prevent the development of these metastases, tumour cells must have disseminated prior to treatment. Currently, no adjuvant therapy has been shown to effectively prevent the outgrowth of metastases. Attention to the patient's psychological state is, therefore, an important aspect of care (see below).

Management

Once the diagnosis is established, the management of patients with UM depends on several factors, including tumour size, location and related features such as retinal detachment, vitreous haemorrhage and retinal invasion[182,184,227]. Other considerations include patient age, general health, status of the opposite eye and the patient's personal desires. All ocular oncology centres should have facilities for radiotherapy and enucleation. Other, more specialized, centres offer local resection and methods of laser treatment, including transpupillary therapy, photodynamic therapy and, more recently, Aura AU-011 nanoparticle therapy[228]. Brachytherapy and enucleation are the most common treatment modalities for UM worldwide, whereas other globe-sparing treatments such as proton beam and resection are additional available therapies. However, as this is a rare tumour, few comparisons between treatment options have been made, and no algorithm or standardized care pathway has been defined. Furthermore, cost and local availability of different modalities at a particular centre are major factors determining the treatment (BOX 4).

Early debate as to whether irradiation can kill all tumour cells[229] and whether enucleation can lead to dissemination of tumour emboli and compromised survival[98] was settled by the Collaborative Ocular Melanoma Study (COMS) trial in 1,317 patients with medium-sized UM (height 2.5–10 mm, largest basal tumour diameter (LBD) no more than 16.0 mm). This showed that the 5-year and 12-year UM-related mortality rates were not significantly different between the two forms of treatment[230,231]. The study justified the use of plaque radiotherapy rather than enucleation for most medium-sized UMs. For large-sized UMs (height >10 mm and LBD >16 mm), a trial in 1,003 patients showed that the 10-year UM-related mortality was not significantly different between enucleation alone and enucleation preceded by external beam radiotherapy[232]. Hence, pre-enucleation radiotherapy has been abandoned. Further large-cohort studies have specifically evaluated plaque radiotherapy for juxtapapillary choroidal UMs[233], for iris melanoma[234], for small choroidal melanoma[188], for large-sized UMs[189] and for extrascleral extension[235]. As the placement of juxtapapillary plaques can be difficult for less experienced ocular oncologists, teletherapy with different radioactive modalities could be another option for juxtapapillary UMs or those located at or near the posterior pole.

Radiotherapy

Radiotherapy is the most common globe-conserving therapy for UM. There are two basic types of radiotherapy: brachytherapy (plaque radiotherapy) and teletherapy (charged particle radiotherapy or stereotactic radiotherapy). With careful patient selection and an experienced physician, there is likely to be no difference in tumour control and treatment complications between plaque radiotherapy, charged particle radiotherapy and stereotactic radiotherapy, but no direct comparisons have been performed. Radiation retinopathy, papillopathy, haemorrhage, cataract, macular oedema, retinal detachment and neovascular glaucoma can occur, especially with large and/or juxtapapillary tumours, and these may require enucleation in some patients[228,234,236,237]. Adverse effects can often be treated with intravitreal injections of steroids or anti-angiogenic agents, laser therapy or resection of the offending nidus in those with so-called toxic tumour syndrome[238].

Plaque radiotherapy. Plaque radiotherapy is a form of brachytherapy that uses several radioisotopes including iodine-125, ruthenium-106, palladium-103, iridium-192 and cobalt-60 (REFS[182,227,239,240]). This treatment involves suturing a curvilinear radioactive plaque onto the sclera, precisely over the tumour, to deliver trans-scleral radiation to the UM. The apex dose of 70 Gy is typically reached after 5 days, when the device is removed.

Toxic tumour syndrome
Radiation vasculopathy within the tumour that results in vascular obstruction and incompetence, leading to ischaemia, neovascular complications, fluid leakage, macular oedema and retinal detachment.

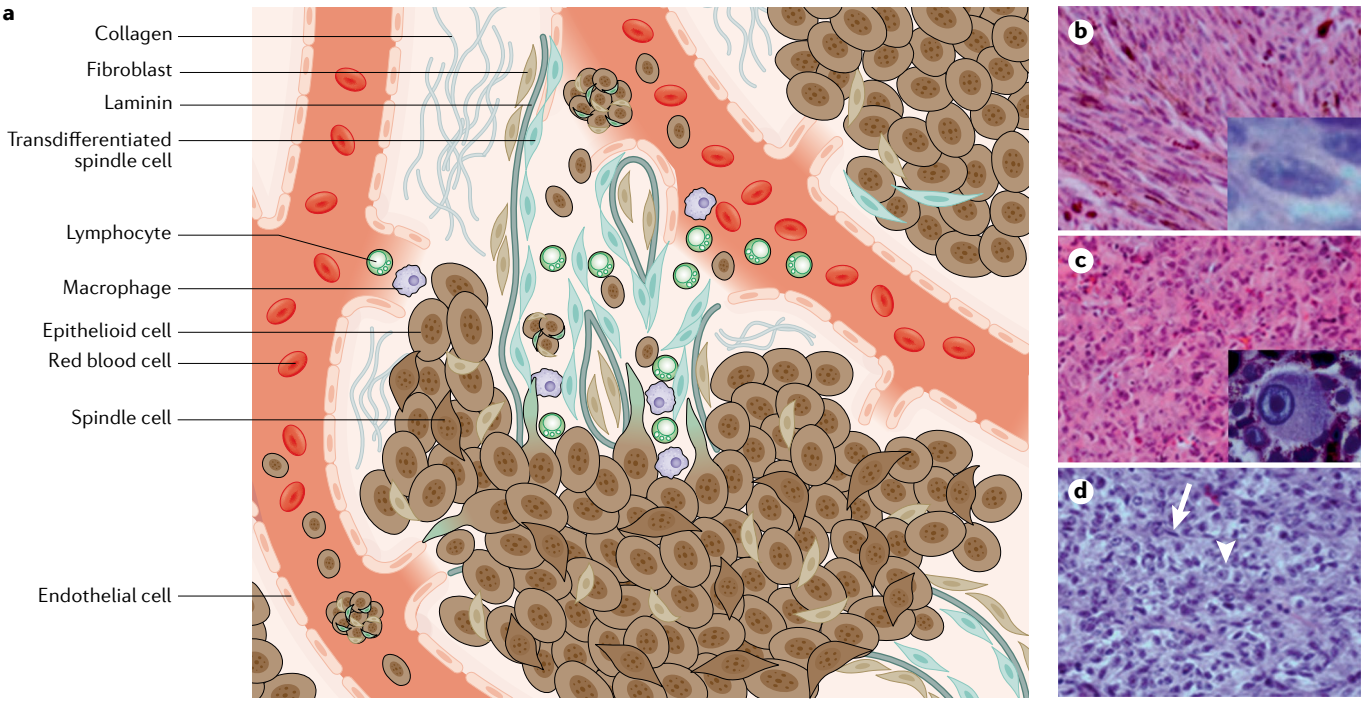

Fig. 9 | **Cell composition in UM. a** | Uveal melanomas (UMs) are composed of a large population of malignant tumour cells and a small extracellular matrix component. UM contains spindle-shaped and epithelioid-shaped tumour cells, endothelial-lined vascular channels (as well as vasculogenic mimicry patterns, whereby cancer cells generate structures that may allow flow of fluids) that are lined at least in part by purportedly transdifferentiated UM cells and fibroblasts. The extracellular matrix includes collagen and laminin. Inflammatory cells, including macrophages and lymphocytes, are typically present. **b** | Based on the cellular morphology, UMs can be classified as spindle-type when at least 90% of the cells are so-shaped. Spindle UM cells have a fusiform nucleus and a prominent nucleolus (inset; ×250, haematoxylin and eosin staining). **c** | UM are classified as epithelioid-type when at least 90% of the cells are so-shaped. Epithelioid UM cells are larger cells with a central, round nucleus and a large nucleolus (inset; ×250, haematoxylin and eosin staining). **d** | UM are classified as mixed when the proportion of cells falls outside these limits. Mixed cell type UM, the most common, is composed of spindle (arrow) and epithelioid (arrowhead) cells (×100, haematoxylin and eosin staining).

The total time depends on the radioactive activity of the plaque. To minimize radiation morbidity, intravitreal steroids or anti-angiogenic agents are offered[236,241]. In expert hands and with careful patient selection, plaque radiotherapy can achieve tumour control in up to 98% of eyes, with globe salvage in ~95% of patients, often with useful vision retention[242,243]. This treatment can be applied to small as well as large UMs (FIG. 11).

Charged particle radiotherapy. Charged particle radiotherapy is a form of teletherapy whereby a finely collimated beam of protons or helium ions delivers a uniform radiation dose to the tumour while minimizing collateral damage to surrounding tissues (Bragg peak effect)[237,244–246]. Tumour control is achieved in 95–98% of eyes[237]. Proton beam radiotherapy has also been used successfully to treat iris melanomas[246].

Stereotactic radiotherapy. With stereotactic radiotherapy, multiple beams of photons are focused onto the tumour from different directions, either simultaneously or sequentially, such that a high dose of radiation is delivered to the tumour while minimizing collateral damage to healthy surrounding tissues[247]. For example, there is growing interest in image-guided, CyberKnife robot-assisted radiosurgery[248].

Laser methods

Laser photocoagulation using xenon arc, argon and infrared diode laser offers control for small tumours, but has largely been abandoned in jurisdictions where radiation is available, owing to the risks of retinal traction, gliosis and tumour recurrence. Other options include transpupillary thermotherapy and photodynamic therapy.

Transpupillary thermotherapy. Transpupillary thermotherapy, in which an infrared laser is used to directly target a tumour through the pupil, was originally developed to decrease the size of a UM prior to irradiation[249]. Currently, the treatment is limited to small pigmented melanomas in the extramacular, extrapapillary region. Early analysis of 256 tumours treated with transpupillary thermotherapy showed control in >90% of tumours[250]. Later analysis of 391 small UMs treated by transpupillary thermotherapy demonstrated that 5 years after treatment, 29% of tumours recurred; lesions with only a few risk factors for UM (rather than naevi) showed better control than those with many risk factors[251]. Indeed, as only small and flat UMs can be treated by transpupillary thermotherapy, many treated lesions are probably naevi. The first series of tumours treated with combined transpupillary thermotherapy and plaque irradiation (so-called sandwich therapy) showed a reduced number

Rhegmatogenous retinal detachment
In which a tear in the retina leads to fluid accumulation and separation of the neurosensory retina from the underlying retinal pigment epithelium.

Snellen lines
The Snellen chart has eleven lines of block letters used to measure visual acuity.

of recurrences[249], but a recent update of a larger series from this centre did not confirm this finding[252].

Photodynamic therapy. In photodynamic therapy, a non-thermal laser activates a photosensitive dye (verteporfin) to induce vascular closure, tumour necrosis and apoptosis. Tumour pigmentation often interferes with this treatment, and it has been proposed that this therapy be added to irradiation specifically in amelanotic tumours[253]. Several small studies have found melanoma control in selected patients[254–256]. A new treatment using an infrared dye-conjugated virus-like particle (AU-011) is under investigation for use in small choroidal melanomas[257,258].

Surgery

Local resection. Local resection of UM involves surgical tumour removal either en bloc through a scleral trapdoor (exoresection) or in a piecemeal fashion with a vitreous cutter passed through the retina (endoresection). These methods are deployed for circumscribed tumours that are considered unsuitable for radiotherapy owing to their large size or juxtapapillary location[259,260]. In addition to tumour removal, resection provides tissue for diagnostic confirmation and prognostication with preservation of the globe and vision[261,262]. However, resection is performed at only a few ocular oncology centres owing to technical difficulty. Complications include rhegmatogenous retinal detachment, haemorrhage and tumour recurrence. Owing to concerns regarding tumour seeding, endoresection is performed only after neoadjuvant radiotherapy in some centres[263]; however, after endoresection alone, rates of local tumour recurrence and metastasis are similar to those reported after other forms of therapy[264].

Enucleation. Enucleation is indicated for advanced UMs (diameter >20 mm, thickness >12 mm), UMs with optic nerve involvement (which are rare) or orbital invasion and/or eyes with secondary glaucoma[182,227]. An orbital implant replaces the globe volume, and some implants can be attached to the rectus muscles so that motility of the prosthesis is retained.

Exenteration. Orbital exenteration (which involves removal of the globe, muscles, nerves and fatty tissue adjacent to the eye) is indicated for cases with massive orbital tumour growth. If possible, the eyelid-sparing exenteration technique is performed to facilitate rapid rehabilitation.

Aftercare

Following ocular treatment of UM, patients are often monitored by an ophthalmologist specialized in ocular oncology. Following irradiation, visits typically take place every 3–6 months for the first 2 years and every 6–12 months thereafter to identify and treat tumour recurrence and any iatrogenic complications[227,265]. At each visit, a full ocular examination is performed, with visual acuity measurement, tonometry (to determine the intraocular pressure) and mydriasis (to enhance examination of the back of the eye). Assessing local tumour control with colour photography and ultrasonography is also required; OCT and, in some cases OCT angiography, are used to identify any maculopathy. Wide-field imaging is useful, using colour photography and fluorescein angiography, to assess for peripheral tumours and retinal perfusion after radiotherapy.

Local recurrence. Local control of UM is high following radiotherapy. In one centre, the rate of recurrence following brachytherapy was 10%, with most recurrences occurring within 5 years of treatment[266]. The most common type of recurrence is at the margin of the tumour, whereas central anterior 'ring' and extraocular extension recurrences are less common. Following plaque radiotherapy, recurrence was 6% at 5 years and 11% at 10 years for small (≤3 mm thickness) UMs, and 13% at 5 years for large (≥10 mm thickness) UMs[188,189]. Recurrence is associated with an increased risk of developing metastases[267]. Recurrence has to be differentiated from inadequate tumour regression (non-responsiveness).

Visual outcomes. Tumour size and proximity to the optic disc and foveola are exquisitely important in visual outcome. Different types of treatment are associated with different ocular outcomes, but radioactive plaque therapy is used as an example for studying outcome. Following plaque radiotherapy for macular UM in 630 eyes, complications at 5 years included visually significant maculopathy (40% of eyes), cataract (32%) and papillopathy (13%)[268]. In a group of 1,106 patients with an initial visual acuity of 20/100 or better, moderate loss of visual acuity of ≥5 Snellen lines was found in 33% at 5 years and 69% at 10 years[242]. Factors predictive of vision loss included

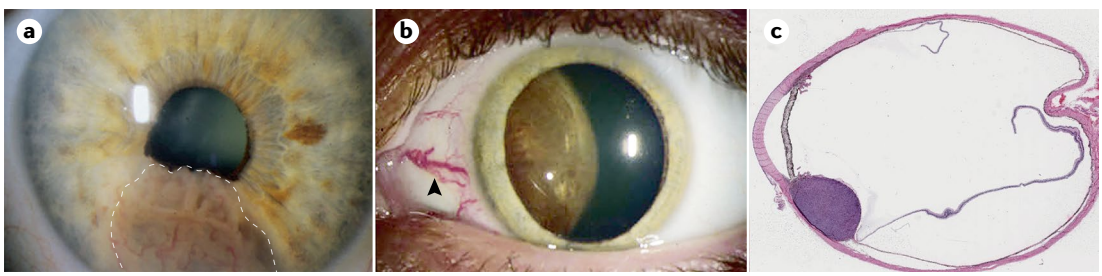

Fig. 10 | **Iris and ciliary body uveal melanoma. a** | Slit lamp photograph shows a vascularized moderately pigmented iris melanoma (dashed line) located in the inferior iris. **b** | Slit lamp photograph shows a pigmented ciliary body melanoma behind the lens, with sentinel vessels in the episclera overlying the tumour (arrowhead). **c** | Low power magnification shows the ciliary body location of a moderately pigmented melanoma (haematoxylin and eosin staining).

Box 4 | **UM treatment worldwide**

Ruthenium brachytherapy is used to treat uveal melanoma (UM) in Argentina, Asia (South Korea and Thailand), many parts of Europe, Iran, South Africa and the United Arab Emirates, with good tumour control and minimal need for enucleation. Iodine brachytherapy can also be used to treat UM and is available in certain places, including Canada, China and New Zealand. Ruthenium and iodine are available in Brazil, Finland, India, Spain and the USA.

Some centres in France, Germany, Italy, South Korea, Poland, Scotland, the USA and Netherlands, offer proton beam therapy for UMs that present with optic nerve infiltration and trans-scleral growth. Unfortunately, this therapy is extremely expensive and not widely available[357]. Various forms of stereotactic radiotherapy have been reported as effective treatment modalities elsewhere in the world[358,359].

Photodynamic therapy has been reported as a treatment for both pigmented and non-pigmented choroidal melanoma in a few centres in Italy[360] and the UK[361]. In the British study, small pigmented lesions were controlled by three sessions in 62% of patients.

Local resection and endoresection have been used for decades as a primary treatment or following radiotherapy with brachytherapy or proton beam[362]. Reports of primary endoresection are available from the UK[264], Russia[363], Iran, Spain, South Africa[364] and Brazil[365].

tumour proximity to the foveola (≤5 mm), greater tumour thickness, poor initial visual acuity, older age (≥60 years) and presence of subretinal fluid[242,269]. For small choroidal tumours (≤3 mm thickness, mean 3 mm to the foveola), poor visual outcome of ≤20/200 at 10 years was noted in 54% of eyes[188], whereas for large UMs (≥10 mm thickness, mean 6 mm to the foveola) poor visual outcome at 7 years was noted in 47% of eyes[189]. Predictors of visual outcome after proton beam radiotherapy are similar[246]. More recently, to minimize radiation complications and improve visual acuity, additional periocular or intravitreal injection of triamcinolone (a glucocorticoid) or intravitreal anti-VEGF agents, and/or sector pan-retinal photocoagulation have been performed[236,241,270,271]. Although the peak development of radiation retinopathy occurs by 5 years, 7% of patients had developed retinopathy 7–10 years after treatment[269]. Thus, extended monitoring for radiation retinopathy is recommended.

Probability of developing metastasis

Systemic surveillance is generally performed to detect metastases, especially after enucleation, and is usually undertaken by a medical oncologist. Surveillance guidelines have been prepared by the US National Comprehensive Cancer Network[265]. Nowadays, a personalized prognostication based on several clinical and genetic determinants can provide accurate prognostic information for each patient[272]. Such prognostic factors are clinical, histological or genetic.

Estimation of metastatic risk is required for patient counselling, planning of systemic surveillance and selection of patients for any available clinical trials of systemic adjuvant therapy. Some highly specialized centres provide adjuvant therapy for patients with high-risk UM to prevent metastatic disease[273], but there is as yet no proof of effectiveness. The frequency and type of any surveillance imaging may be stratified according to risk. The standard prognostic tool for choroidal and ciliary body UMs is the AJCC TNM staging system[267], which is based on evidence from >7,000 patients provided by members of the European Ophthalmic Oncology Group. First, tumours are categorized according to their basal diameter and thickness, then sub-categorized according to ciliary body involvement, extraocular extension or both. These categories are grouped into stages I–IV according to their statistical association with metastatic mortality, the 10-year survival probability being ~90% for those with AJCC stage I tumours, ~75% for those with stage II tumours and <60% for those with stage III tumours[267].

A limitation of the AJCC staging system is that it does yet not take into account tumour histology and genetic characteristics. Histopathological predictors of metastases include epithelioid cell type, high number of mitoses[274], presence of high numbers of lymphocytes or macrophages[159,275] and presence of specific extravascular matrix patterns[226]. Genetic markers of a bad prognosis are monosomy 3 and the presence of additional copies of chromosome 8 (REFS[276–278]), whereas 6p gain provides a protective effect[279,280]. Genetic studies have shown that analysis of the chromosome status[281,282], mutation type[101] or the mRNA GEP[20,283] can be used for prognostication (reviewed in REF.[284]). Based on cytogenetics analysis in 1,059 patients, tumours with monosomy 3 and 8q gain demonstrate an 11–123-fold increased risk of metastatic disease compared with tumours with normal chromosomes 3, 6 and 8 (REF.[216]). Combining cytogenetics analysis with the AJCC tumour classification in a group of 522 patients provided a significant improvement in prognostication[285,286]. Based on the GEP of tumour mRNA instead of chromosome status, tumours can be divided into class I and class II tumours: in 459 patients, the 4-year risk of metastasis was 3% for class I GEP and 80% for class II GEP[287]. Class I GEP corresponds to a normal chromosome 3 status (tumour types A and B; TABLE 1), and class II GEP to monosomy 3 (tumour types C and D; TABLE 1)[18–20]. A further subdivision of class I is possible, with class Ib having a worse prognosis than class Ia.

Aside from tumour size and genetics, a wide range of patient and tumour characteristics influence the development of metastases. The Liverpool Uveal Melanoma Prognosticator Online (LUMPO) estimates both metastatic and non-metastatic mortality according to anatomical, pathological and genetic factors, also taking patient age and sex into account[281,288] (FIG. 1 2). The model adjusts for bias caused by missing data and competing risks and is available on the Internet, currently free of charge. This tool is evolving as more data accrue. The latest version, LUMPO III, includes 8q gains in the model and recently underwent multicentre validation. A different online tool, PRiMeUM, can predict metastases within 48 months of treatment of a primary UM[289].

The reliability of prognostication depends on the accuracy of tumour measurements and, if tissue is available, the subjective categorization of histological findings as well as the sensitivity of genetic analyses. As with other diseases, prognostication takes account of how much the patient wishes to know and is supported by adequate counselling and psychological support.

Treatment for metastasis

Consensus statements by the National Comprehensive Cancer Network and other organizations recommend consideration of surveillance, including imaging of the liver, based upon metastatic risk, with broad latitude

regarding imaging modality (based upon local expertise), frequency (3–12 month intervals) and duration (10 years, then subsequently as clinically indicated)[265,290]. Hepatic MRI is frequently used for surveillance; however, it should be noted that small metastatic tumours with pseudosinusoidal spaces are camouflaged within the surrounding tissue so that they may not be detected by MRI[122]. The nodular pattern is vascularized and may be more evident with this imaging modality[291].

As there is no standard treatment for the prevention or treatment of metastases, clinical trial participation is encouraged for patients in both adjuvant and advanced disease settings, although the number of trials developed specifically in UM remains low. In the adjuvant setting, no survival benefit was observed in patients with UM treated with interferon in two single-arm trials when compared with historical controls[292,293]. Two completed randomized adjuvant trials in this disease were similarly negative, one with dacarbazine and another with Bacillus Calmette-Guérin injections[294,295]. Contemporary adjuvant trials limit eligibility to patients at high-risk of developing metastasis based upon clinical and/or molecular prognostic factors, reducing the sample size required; however, enrolment remains challenging as highlighted by FOTEAD, a randomized phase III trial of adjuvant fotemustine versus observation, which closed prematurely due to slow accrual[296]. Once metastatic disease has developed, options include observation or participation in trials. No curative treatment has been identified and, as UM differs from cutaneous melanoma, trials should be UM-specific[1]. Currently active trials are based on biological insights in UM that suggest critical roles for the PKC–MAPK signalling pathway, epigenetic modifications, angiogenesis and immunology (TABLE 2).

Surgical resection or ablation of oligometastases may improve outcome in selected patients. As liver metastases are preferentially supplied by hepatic artery branches, regional approaches, including intra-arterial chemotherapy, isolated hepatic perfusion and chemoembolization, have been investigated. Two randomized phase III trials of liver-directed therapies including patients with UM have been completed, including one comparing hepatic intra-arterial with intravenous fotemustine ($n = 171$)[297] and another comparing melphalan percutaneous hepatic perfusion (PHP) with best alternative care ($n = 93$)[298]. Both approaches demonstrated improved responses and disease control with regional therapy, with no effect on survival; however, the melphalan trial permitted crossover of patients initially randomly assigned to best alternative care to receive PHP at the time of progression, confounding the analysis of survival effects. The ongoing phase III FOCUS trial was initially designed to randomly assign 240 patients to PHP or best alternative care without crossover, with a primary end point of survival; however, due to accrual challenges, the study was modified to remove random assignment.

Various systemic treatments have been evaluated primarily in single-arm phase II studies, with response rates generally <10%, disease control of <4 months and survival of <1 year. Systemic chemotherapeutic regimens in UM have been adopted from cutaneous melanoma, including dacarbazine, temozolomide, cisplatin, bendamustine, treosulfan, fotemustine-based regimens and others, without meaningful clinical improvement[299–306]. Inhibition of pathways downstream of $G\alpha_q$ at the level of MEK or PKC alone and in combination with components of the AKT–PI3K pathway have been studied, with limited, if any, benefit achieved for the overall population[307–309]. However, clinical benefit was observed in smaller subsets of patients in some studies[310], which may not be reflected in the reported clinical end points, which are typically reported as median values. Additional strategies targeting downstream effectors of $G\alpha_q$[79,80], $G\alpha_q$ directly[311] and epigenetic modifications[18,312,313] have demonstrated preclinical efficacy, providing rationale for additional ongoing studies (TABLE 2). Immune checkpoint blockade at the level of CTLA4 (REFS[314,315]) or PD1 (REF.[316]) demonstrated response rates of <10% and was associated with a median survival of <1 year. The high mutational burden that may develop in patients with UM harbouring biallelic loss of *MBD4* may result in a few patients achieving significant clinical benefit with single-agent checkpoint blockade[42], but, in general, the clinical utility of these agents in the unselected UM population is poor. Outside clinical trials, combinatorial checkpoint blockade has achieved numerically superior response rates and survival when compared with historical controls, and such therapy is a reasonable consideration for patients who can tolerate the potential adverse effects[317]. Additional novel immunological strategies, including adoptive T cell therapy[177] and T cell redirection[181] have also demonstrated promising preliminary results, and tebentafusp (IMCgp100), a bispecific molecule targeting

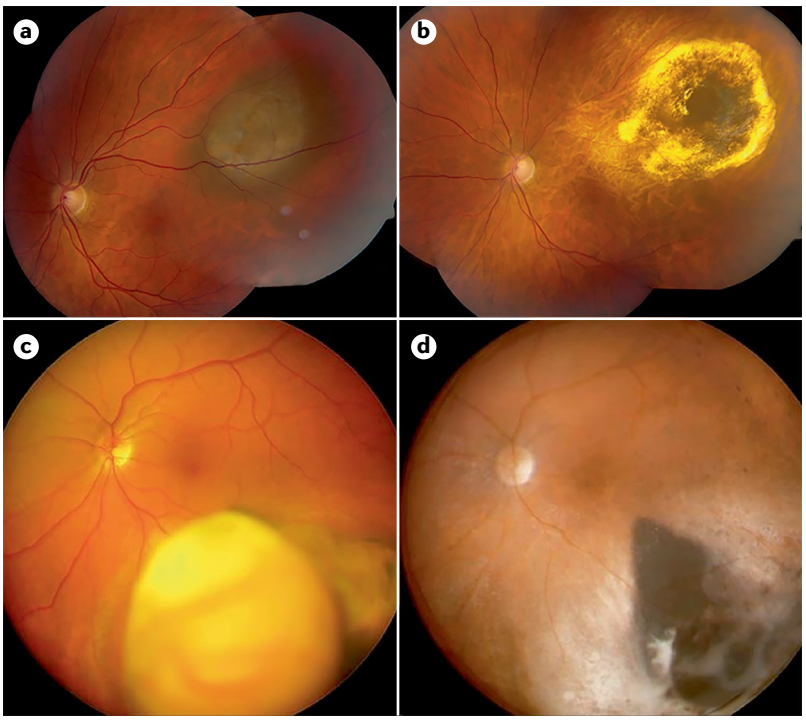

Fig. 11 | **A medium-sized and a large choroidal melanoma before and after irradiation. a** | A medium-sized choroidal melanoma (thickness 5.0 mm) before irradiation. **b** | The same tumour as in panel **a** after radioactive plaque irradiation (thickness 2.0 mm). **c** | A large choroidal melanoma (thickness 9.0 mm) before irradiation. **d** | The same tumour as in panel **c** after plaque radiotherapy (thickness 3.5 mm).

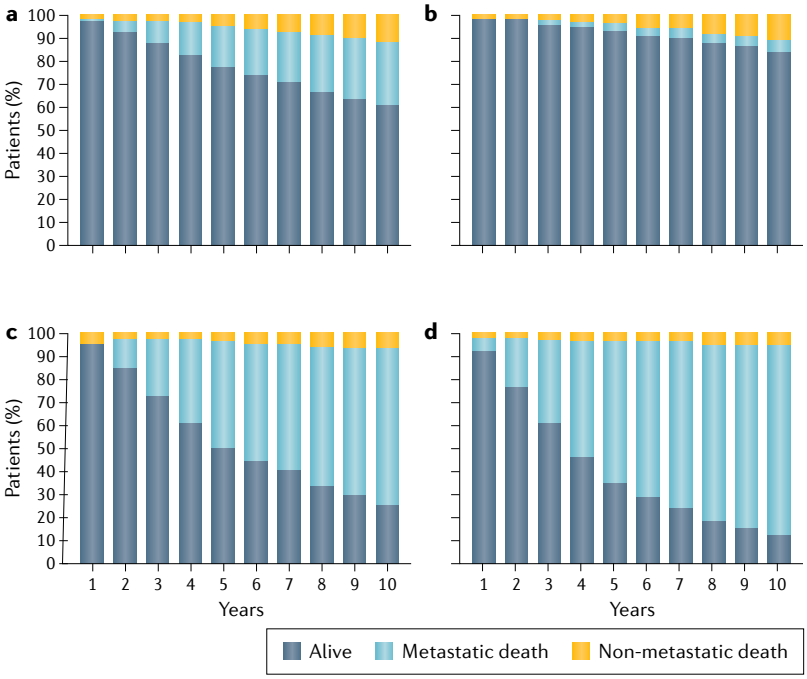

Fig. 12 | **LUMPO prognostication tool.** The Liverpool Uveal Melanoma Prognosticator Online LUMPO III estimates of survival, metastatic death and non-metastatic death in a woman 60 years of age with a choroidal melanoma with a basal diameter of 16 mm and a thickness of 8 mm if: no histological and no genetic data are available (panel **a**); no epithelioid cells are present, and the tumour has no chromosome 3 loss and no 8q gain (panel **b**); epithelioid cells are present and the tumour has monosomy 3 alone (panel **c**); and if epithelioid cells are present, and the tumour has both monosomy 3 and 8q gain (panel **d**). The statistical model adjusts for competing risks. This figure shows the value of prognostic tumour biopsy. Developed using the LUMPO III prototype (www.LUMPO.net), and adapted with permission from Azzam Taktak, Royal Liverpool University Hospital, Liverpool, UK and Bertil Damato, Nuffield Department of Clinical Neurosciences, University of Oxford, UK.

gp100 and that attracts CTLs to the UM cells, is now in registration-intent development[318,319].

Quality of life

Patient-reported outcomes

After ocular treatment, patients with posterior UM can experience ocular discomfort, visual difficulties, facial deformity after exenteration, worries about future health, anxiety, depression and/or loss of wellbeing. Awareness of these problems has improved patient counselling, treatment selection and psychological support aimed at preventing or alleviating any distress.

The largest study on quality of life to date was performed at the Liverpool Ocular Oncology Service, UK. It included 442 patients who had undergone primary enucleation and 1,154 patients who had received ruthenium plaque radiotherapy or proton beam radiotherapy[320]. Patients who underwent enucleation were more likely to be male and older, and had a more advanced tumour and a poorer survival probability. After enucleation, almost one-third of patients reported difficulties caused by loss of stereopsis and visual field. Over time, these difficulties diminished as the patients adjusted to their monocularity, but worsened in patients who had received radiotherapy, owing to increasing radiation-induced morbidity[321]. This information is useful in personalizing care.

Stereopsis
Depth perception.

Worries about future metastasis were more common after enucleation than radiotherapy (36% versus 29%)[320]. Worries about local tumour recurrence were reported by 22% of irradiated patients and, interestingly, by 18% of patients who underwent enucleation. This surprising finding emphasizes the need for repeated counselling and reassurance[320]. Multivariable analyses showed minimal differences between the two kinds of treatment with respect to anxiety, depression and wellbeing, which were more likely to be determined by age, sex, general health, social support, employment and other factors unrelated to the ocular tumour or its treatment. These insights should enhance the counselling that is provided to patients when deciding between enucleation and radiotherapy. Fewer than 20% of patients reported their quality of life to be 'poor' and, of these, only 20% attributed their poor quality of life to their ocular condition. Indeed, the wellbeing of the patients in this UK study was comparable to that of the general US population, except for emotional wellbeing, which was found to be poorer after enucleation, probably owing to fears of developing metastatic disease. These data are useful to ensure practitioners provide sensitive reassurance to patients. These results indicate that patients with UM experience good quality of life, even after enucleation, but may need psychological support if they encounter adversity, such as a high-risk of metastasis, poor general health, poor vision in the opposite eye or lack of social support. Economic implications of these findings have not been studied but may result in financial savings if the data from this study encourage patients with advanced disease to have primary enucleation, thereby avoiding a prolonged course of treatment for radiation-induced complications.

Patient needs and satisfaction with care

An online survey of patients with UM by the Ocular Melanoma Foundation in the USA about their expected care revealed a number of shortcomings[322]. Patients expressed regret that their tumour had not immediately been detected, that they had not been informed of the presence of a fundus lesion and that they were not advised that the 'mole' that was being observed without treatment could be malignant. Other complaints included the 'callous' manner in which patients were spoken to by their ophthalmologist, lack of emotional support, lack of opportunity to ask questions, insufficient information regarding all therapeutic options and lack of awareness regarding prognostic biopsy. Patients also indicated that they would have liked more information and advice on matters such as financial implications of investigations and treatment, patient advocacy groups and how to discuss their condition with their family, friends and colleagues at work.

The authors of the study prepared a 'bill of rights' specific to patients with UM, which included the right to be informed of any findings and their significance, to be informed of all therapeutic options (including those not available at the treatment centre) and to be informed of what to expect should they decide not to have a treatment. Furthermore, each patient should have the opportunity to ask questions and to be informed of

the option of having a prognostic biopsy and genetic tumour typing, with an adequate explanation of the risks and benefits of this procedure. Although such standards apply to all patients with any disease, the hope is that this bill of rights will improve standards of care for patients with UM, especially in centres where patients are not managed by ocular oncologists in an experienced multidisciplinary team and in departments that lack necessary imaging and therapeutic resources. In time, patient advocacy groups may define minimum specifications for ocular oncology clinics, even publicly 'naming and shaming' health-care providers and departments that fall short of expectations. Defining the specifications for ocular oncology fellowships will help to further educate ophthalmologists with an interest in ocular oncology.

Outlook

Although the main oncogenic events in primary UM are known, a better understanding of their sequence and biological consequences is needed to effectively prevent or treat metastases. What the consequences are of *BAP1* inactivation, aberrant splicing in *SF3B1* or aberrant translation in *EIF1AX* remain to be determined. How the recurrent copy number alterations found in most UM, such as monosomy 3 and/or gain of 8q, drive tumorigenesis also remains unclear. Recent studies have shown that many genetic aberrations are similar in the primary and the metastases[105,106]; accordingly, information about these abnormalities may help develop therapies for metastatic disease. However, metastases also harbour additional mutations, which may be targets for therapy. Accordingly, approaches that cause DNA damage to increase the mutational burden of the tumour, prior to applying immunotherapy, may have merit in UM[323–325].

We furthermore need a better understanding of interactions between tumour cells and their microenvironment, both in the primary disease and metastatic setting, to determine which drugs or which forms of immunotherapy might be effective, and what can be done to overcome the current lack of effect of many immunological approaches. We need to know whether the relative resistance to immune checkpoint blockade in UM may

Table 2 | **Clinical trials for patients with advanced uveal melanoma in 2020**

Agent	Phase	Sponsor	ClinicalTrials.gov ID
Adjuvant trials			
Sunitinib versus valproic acid	II	Thomas Jefferson University (Philadelphia, PA, USA)	NCT02068586
Dendritic cells plus autologous tumour RNA	III	University Hospital Erlangen (Erlangen, Germany)	NCT01983748
Ipilimumab and nivolumab	II	Georgetown University (Washington, DC, USA)	NCT03528408
PKC–MAPK pathway			
Intermittent selumetinib	I	Columbia University (New York, NY, USA)	NCT02768766
IDE196	I/II	IDEAYA Biosciences (San Francisco, CA, USA)	NCT03947385
Epigenetic therapies			
Vorinostat	II	National Cancer Institute (Bethesda, MD, USA)	NCT01587352
PLX2853	I/II	Plexxikon (Berkeley, CA, USA)	NCT03297424
DNA damage repair targeting			
Neratinib	II	University of Florida (Gainesville, FL, USA)	NCT03207347
Immune checkpoint blockade			
Ipilimumab plus nivolumab and immunoembolization	II	Thomas Jefferson University (Philadelphia, PA, USA)	NCT03472586
Ipilimumab plus nivolumab and yttrium-90 radioembolization	0	California Pacific Medical Center (San Francisco, CA, USA)	NCT02913417
ADV/HSV-tk, stereotactic body radiation therapy and nivolumab	II	Houston Methodist Hospital (Houston, TX, USA)	NCT02831933
Cellular therapy			
Dendritic cell vaccine	II	University Hospital Erlangen (Erlangen, Germany)	NCT01983748
Adoptive T cell therapy	II	University of Pittsburgh (Pittsburgh, PA, USA)	NCT03467516
Cellular adoptive immunotherapy plus ipilimumab	I	MD Anderson Cancer Center (Houston, TX, USA)	NCT03068624
T cell redirection			
Tebentafusp (IMCgp100)	II	Immunocore Ltd (Milton, UK)	NCT03070392
Hepatic intratumoural and regional therapies			
Radioembolization versus transarterial chemoembolization	II	Charité – Universitätsmedizin Berlin (Berlin, Germany)	NCT02936388
Isolated hepatic perfusion versus best alternative care	III	Sahlgrenska University Hospital (Gothenburg, Sweden)	NCT01785316
Percutaneous hepatic perfusion	III	Delcath Systems Inc. (Queensbury, NY, USA)	NCT02678572
Intratumoural PV-10	I	Provectus Biopharmaceuticals Inc. (Knoxville, TN, USA)	NCT00986661

Actively recruiting on 18 January 2020; see www.clinicaltrials.gov for a real-time listing. ADV/HSV-tk, adenovirus/herpes simplex virus thymidine kinase.

partly be attributable to expression of checkpoint molecules other than PDL1, and further clarity is required regarding the immune cells involved in UM, mechanisms of immune evasion unique to UM, and clinical and molecular predictors of benefit to immunotherapies. Indeed, tebentafusp, which redirects $CD3^+$ T cells to gp100-expressing UM cells, has shown promising preliminary clinical efficacy, which may reflect the need to draw T cells to the tumour. Despite the limited efficacy of immune checkpoint blockade in UM, the early clinical results of tebentafusp suggest that UM requires immune modulation different from that required in, for example, cutaneous melanoma, for optimal antitumour effects.

From a clinical perspective, early detection of ocular tumours is improving through advances in ocular imaging in the community; however, differentiation of small UMs from naevi and other benign lesions continues to be a problem. Overcoming these difficulties by applying artificial intelligence to ocular imaging may be possible and is already happening with other diseases. Furthermore, prognostication has improved substantially through the use of multivariable analysis that includes anatomical, histological and/or genetic predictors, in combination with age and sex. Novel statistical methods can overcome bias caused by missing data and competing causes of death. Such progress is expected to continue with further advances in biopsy, genetics and statistics.

Once diagnosed, the goals of treatment of the primary tumour are to prevent metastatic spread and to conserve the eye with useful vision. However, no standardized management algorithm is available. Although saving the eye is usually possible with radiotherapy, vision often deteriorates with posterior UMs owing to radiation-induced optic neuropathy and maculopathy. Ocular morbidity can also occur as a result of exudation from the irradiated tumour and excessive production of angiogenic factors, which can cause optic disc and iris neovascularization and neovascular glaucoma (toxic tumour syndrome). A better understanding of the pathology of such iatrogenic morbidity should improve ocular outcomes. Recent advances in immunotherapy and chemotherapy have enhanced prospects to reduce tumour volume before administering focal ocular therapy, thereby minimizing ocular morbidity.

Many UMs metastasize at a very early stage; micrometastases are already present by the time the tumour is first recognized and treated. This insight has stimulated interest in replacing long-term surveillance of small melanocytic tumours of uncertain malignancy with genetic analysis of tumour or liquid biopsies to enable early treatment[206]. Emerging strategies for treating such tumours with minimal morbidity include photodynamic therapy that is administered by intravitreal injection of a novel, recombinant, papillomavirus-like particle drug (AU-011) conjugated with a phthalocyanine photosensitizer (IRDye 700DX)[258]. This conjugate is then activated by a near-infrared laser, causing a cytotoxic tumour effect. This drug is currently under investigation for safety and efficacy in the treatment of small choroidal melanoma[257].

Several studies have shown that local failure of UM treatment is associated with a higher rate of metastatic disease[326]. Whether the persistent tumour causes metastasis or whether recurrence is only an indicator of increased malignancy is not known. To address this question, studies are being planned to compare the genetic profiles of recurrent tumours with pretreatment biopsies, which may enable ocular treatment to be tailored not only according to tumour size and location but also histological and genetic 'degrees' of malignancy.

Awareness is growing of the need to provide more holistic care, not only treating the disease but also providing better psychological support to patients and their families. These measures are improving the wellbeing of those affected by UM, regardless of outcome. However, the ultimate goal is — of course — to develop treatments that will save vision, effectively treat metastases and, ultimately, save lives.

Published online: 09 April 2020

1. Rodrigues, M. et al. So close, yet so far: discrepancies between uveal and other melanomas. A position paper from UM Cure 2020. *Cancers* **11**, e1032 (2019).
2. Shields, C. L. et al. Iris melanoma: features and prognosis in 317 children and adults. *J. Am. Assoc. Pediatr. Ophthalmol. Strabismus* **16**, 10–16 (2012).
3. Al-Jamal, R. T. et al. The pediatric choroidal and ciliary body melanoma study. *Ophthalmology* **123**, 898–907 (2016).
4. Walpole, S. et al. Comprehensive study of the clinical phenotype of germline *BAP1* variant-carrying families worldwide. *J. Natl Cancer Inst.* **110**, 1328–1341 (2018).
5. Royer-Bertrand, B. et al. Comprehensive genetic landscape of uveal melanoma by whole-genome sequencing. *Am. J. Hum. Genet.* **99**, 1190–1198 (2016).
6. de Lange, M. J. et al. Distribution of GNAQ and GNA11 mutation signatures in uveal melanoma points to a light dependent mutation mechanism. *PLoS One* **10**, e0138002 (2015).
7. Furney, S. J. et al. SF3B1 mutations are associated with alternative splicing in uveal melanoma. *Cancer Discov.* **3**, 1122–1129 (2013).
8. Singh, A. D., Rennie, I. G., Seregard, S., Giblin, M. & McKenzie, J. Sunlight exposure and pathogenesis of uveal melanoma. *Surv. Ophthalmol.* **49**, 419–428 (2004).
9. Sliney, D. H. How light reaches the eye and its components. *Int. J. Toxicol.* **21**, 501–509 (2002).
10. Li, W., Judge, H., Gragoudas, E. S., Seddon, J. M. & Egan, K. M. Patterns of tumor initiation in choroidal melanoma. *Cancer Res.* **60**, 3757–3760 (2000).
11. Damato, E. M. & Damato, B. E. Detection and time to treatment of uveal melanoma in the United Kingdom: an evaluation of 2384 patients. *Ophthalmology* **119**, 1582–1589 (2012).
12. Kujala, E., Mäkitie, T. & Kivelä, T. Very long-term prognosis of patients with malignant uveal melanoma. *Invest. Ophthalmol. Vis. Sci.* **44**, 4651–4659 (2003).
13. Jensen, O. A. Malignant melanomas of the human uvea: 25-year follow-up of cases in Denmark, 1943–1952. *Acta Ophthalmol.* **60**, 161–182 (1982).
14. Damato, B. Ocular treatment of choroidal melanoma in relation to the prevention of metastatic death – a personal view. *Prog. Retin. Eye Res.* **66**, 187–199 (2018).
15. Vader, M. J. C. et al. GNAQ and GNA11 mutations and downstream YAP activation in choroidal nevi. *Br. J. Cancer* **117**, 884–887 (2017).
This study showed that most regular choroidal naevi carry a mutation in *GNAQ* or *GNA11*.
16. Van Raamsdonk, C. D. et al. Frequent somatic mutations of GNAQ in uveal melanoma and blue naevi. *Nature* **457**, 599–602 (2009).
This paper first identified the role of *GNAQ* mutations in the development of UM.
17. Van Raamsdonk, C. D. et al. Mutations in GNA11 in uveal melanoma. *N. Engl. J. Med.* **363**, 2191–2199 (2010).
18. Robertson, A. G. et al. Integrative analysis identifies four molecular and clinical subsets in uveal melanoma. *Cancer Cell* **32**, 204–220.e15 (2017).
This report describes the use of different platforms to identify four subtypes of UM, each with different genetic, mRNA, long non-coding RNA and epigenetic patterns.
19. Jager, M. J., Brouwer, N. J. & Esmaeli, B. The cancer genome atlas project: an integrated molecular view of uveal melanoma. *Ophthalmology* **125**, 1139–1142 (2018).
This paper defines four categories of UM.
20. Onken, M. D., Worley, L. A., Ehlers, J. P. & Harbour, J. W. Gene expression profiling in uveal melanoma reveals two molecular classes and predicts metastatic death. *Cancer Res.* **64**, 7205–7209 (2004).
Expression of mRNA was used in this study to identify two different patterns, which had prognostic significance and led to the development of a clinical test for the prognostication of UM.
21. Martin, M. et al. Exome sequencing identifies recurrent somatic mutations in EIF1AX and SF3B1 in uveal melanoma with disomy 3. *Nat. Genet.* **45**, 933–936 (2013).
22. Maat, W. et al. Monosomy of chromosome 3 and an inflammatory phenotype occur together in uveal melanoma. *Invest. Ophthalmol. Vis. Sci.* **49**, 505–510 (2008).

23. Harbour, J. W. et al. Frequent mutation of BAP1 in metastasizing uveal melanomas. *Science* **330**, 1410–1413 (2010).
Mutations in a gene on chromosome 3, *BAP1*, were discovered in this work and shown to be associated with the development of metastases in UM.
24. Mazloumi, M. et al. Accuracy of the Cancer Genome Atlas classification vs American Joint Committee on Cancer classification for prediction of metastasis in patients with uveal melanoma. *JAMA Ophthalmol.* **138**, 260–267 (2020).
25. Virgili, G. et al. Incidence of uveal melanoma in Europe. *Ophthalmology* **114**, 2309–2315.e2 (2007).
26. Singh, A. D., Turell, M. E. & Topham, A. K. Uveal melanoma: trends in incidence, treatment, and survival. *Ophthalmology* **118**, 1881–1885 (2011).
27. Baily, C. et al. Uveal melanoma in Ireland. *Ocul. Oncol. Pathol.* **5**, 195–204 (2019).
28. Vajdic, C. M. et al. Incidence of ocular melanoma in Australia from 1990 to 1998. *Int. J. Cancer* **105**, 117–122 (2003).
29. Michalova, K., Clemett, R., Dempster, A., Evans, J. & Allardyce, R. A. Iris melanomas: are they more frequent in New Zealand? *Br. J. Ophthalmol.* **85**, 4–5 (2001).
30. Park, S. J. et al. Nationwide incidence of ocular melanoma in South Korea by using the National Cancer Registry Database (1999–2011). *Invest. Ophthalmol. Vis. Sci.* **56**, 4719–4725 (2015).
31. Tomizuka, T., Namikawa, K. & Higashi, T. Characteristics of melanoma in Japan: a nationwide registry analysis 2011–2013. *Melanoma Res.* **27**, 492–497 (2017).
32. Kivela, T. The epidemiological challenge of the most frequent eye cancer: retinoblastoma, an issue of birth and death. *Br. J. Ophthalmol.* **93**, 1129–1131 (2009).
33. Metzelaar-Blok, J. A. et al. Characterization of melanocortin-1 receptor gene variants in uveal melanoma patients. *Invest. Ophthalmol. Vis. Sci.* **42**, 1951–1954 (2001).
34. Weis, E., Shah, C. P., Lajous, M., Shields, J. A. & Shields, C. L. The association between host susceptibility factors and uveal melanoma: a meta-analysis. *Arch. Ophthalmol.* **124**, 54–60 (2006).
35. van Hees, C. L. et al. Are atypical nevi a risk factor for uveal melanoma? A case-control study. *J. Invest. Dermatol.* **103**, 202–205 (1994).
36. van Hees, C. L., Jager, M. J., Bleeker, J. C., Kemme, H. & Bergman, W. Occurrence of cutaneous and uveal melanoma in patients with uveal melanoma and their first degree relatives. *Melanoma Res.* **8**, 175–180 (1998).
37. Richtig, E., Langmann, G., Müllner, K. & Smolle, J. Ocular melanoma: epidemiology, clinical presentation and relationship with dysplastic nevi. *Ophthalmologica* **218**, 111–114 (2004).
38. Ferguson, R. et al. Genetic markers of pigmentation are novel risk loci for uveal melanoma. *Sci. Rep.* **6**, 31191 (2016).
39. Schmidt-Pokrzywniak, A., Jöckel, K.-H., Bornfeld, N., Sauerwein, W. & Stang, A. Positive interaction between light iris color and ultraviolet radiation in relation to the risk of uveal melanoma. *Ophthalmology* **116**, 340–348 (2009).
40. Mobuchon, L. et al. A GWAS in uveal melanoma identifies risk polymorphisms in the CLPTM1L locus. *NPJ Genomic Med.* **2**, 5 (2017).
41. James, M. A., Vikis, H. G., Tate, E., Rymaszewski, A. L. & You, M. CRR9/CLPTM1L regulates cell survival signaling and is required for Ras transformation and lung tumorigenesis. *Cancer Res.* **74**, 1116–1127 (2014).
42. Rodrigues, M. et al. Outlier response to anti-PD1 in uveal melanoma reveals germline MBD4 mutations in hypermutated tumors. *Nat. Commun.* **9**, 1866 (2018).
43. Johansson, P. A. et al. Prolonged stable disease in a uveal melanoma patient with germline MBD4 nonsense mutation treated with pembrolizumab and ipilimumab. *Immunogenetics* **71**, 433–436 (2019).
44. Huang, K. et al. Pathogenic germline variants in 10,389 adult cancers. *Cell* **173**, 355–370.e14 (2018).
45. Strande, N. T. et al. Evaluating the clinical validity of gene-disease associations: an evidence-based framework developed by the clinical genome resource. *Am. J. Hum. Genet.* **100**, 895–906 (2017).
46. Aoude, L. G., Vajdic, C. M., Kricker, A., Armstrong, B. & Hayward, N. K. Prevalence of germline *BAP1* mutation in a population-based sample of uveal melanoma cases. *Pigment Cell Melanoma Res.* **26**, 278–279 (2013).
47. Gupta, M. P. et al. Clinical characteristics of uveal melanoma in patients with germline *BAP1* mutations. *JAMA Ophthalmol.* **133**, 881–887 (2015).
48. Rai, K. et al. Germline *BAP1* alterations in familial uveal melanoma: BAP1 in familial uveal melanoma. *Genes Chromosomes Cancer* **56**, 168–174 (2017).
49. Wiesner, T. et al. Germline mutations in BAP1 predispose to melanocytic tumors. *Nat. Genet.* **43**, 1018–1021 (2011).
50. Singh, A. D. et al. Familial uveal melanoma. Clinical observations on 56 patients. *Arch. Ophthalmol.* **114**, 392–399 (1996).
51. Abdel-Rahman, M. H. et al. Whole exome sequencing identifies candidate genes associated with hereditary predisposition to uveal melanoma. *Ophthalmology* https://doi.org/10.1016/j.ophtha.2019.11.009 (2019).
52. Lobo, J. et al. Ovarian metastasis from uveal melanoma with MLH1/PMS2 protein loss in a patient with germline MLH1 mutated Lynch syndrome: consequence or coincidence? *Virchows Arch.* **470**, 347–352 (2017).
53. Cruz, C., Teule, A., Caminal, J. M., Blanco, I. & Piulats, J. M. Uveal melanoma and *BRCA1*/*BRCA2* genes: a relationship that needs further investigation. *J. Clin. Oncol.* **29**, e827–e829 (2011).
54. Iscovich, J. et al. Prevalence of the BRCA2 6174 del T mutation in Israeli uveal melanoma patients. *Int. J. Cancer* **98**, 42–44 (2002).
55. Sinilnikova, O. M. et al. Germline brca2 sequence variants in patients with ocular melanoma. *Int. J. Cancer* **82**, 325–328 (1999).
56. Marous, C. L., Marous, M. R., Welch, R. J., Shields, J. A. & Shields, C. L. Choroidal melanoma, sector melanocytosis, and retinal pigment epithelial microdetachments in Birt–Hogg–Dubé syndrome. *Retin. Cases Brief. Rep.* **13**, 202–206 (2019).
57. Fontcuberta, I. C., Salomão, D. R., Quiram, P. A. & Pulido, J. S. Choroidal melanoma and lid fibrofoliculomas in Birt-Hogg-Dubé syndrome. *Ophthalmic Genet.* **32**, 143–146 (2011).
58. Baglietto, L. et al. Risks of Lynch syndrome cancers for MSH6 mutation carriers. *J. Natl. Cancer Inst.* **102**, 193–201 (2010).
59. Abdel-Rahman, M. H., Pilarski, R., Ezzat, S., Sexton, J. & Davidorf, F. H. Cancer family history characterization in an unselected cohort of 121 patients with uveal melanoma. *Fam. Cancer* **9**, 431–438 (2010).
60. Bergman, L., Nilsson, B., Ragnarsson-Olding, B. & Seregard, S. Uveal melanoma: a study on incidence of additional cancers in the Swedish population. *Invest. Ophthalmol. Vis. Sci.* **47**, 72–77 (2006).
61. Hemminki, K. & Jiang, Y. Association of ocular melanoma with breast cancer but not with cutaneous melanoma: results from the Swedish Family-Cancer Database. *Int. J. Cancer* **94**, 907–909 (2001).
62. Collaborative Ocular Melanoma Study Group. Development of metastatic disease after enrollment in the COMS trials for treatment of choroidal melanoma: Collaborative Ocular Melanoma Study Group Report No. 26. *Arch. Ophthalmol.* **123**, 1639–1643 (2005).
63. Scélo, G. et al. Associations between ocular melanoma and other primary cancers: an international population-based study. *Int. J. Cancer* **120**, 152–159 (2007).
64. Nayman, T., Bostan, C., Logan, P. & Burnier, M. N. Uveal melanoma risk factors: a systematic review of meta-analyses. *Curr. Eye Res.* **42**, 1085–1093 (2017).
65. Holly, E. A., Aston, D. A., Ahn, D. K. & Smith, A. H. Intraocular melanoma linked to occupations and chemical exposures. *Epidemiol. Camb. Mass.* **7**, 55–61 (1996).
66. Napolitano, A. et al. Minimal asbestos exposure in germline BAP1 heterozygous mice is associated with deregulated inflammatory response and increased risk of mesothelioma. *Oncogene* **35**, 1996–2002 (2016).
67. Betti, M. et al. Sensitivity to asbestos is increased in patients with mesothelioma and pathogenic germline variants in *BAP1* or other DNA repair genes. *Genes Chromosomes Cancer* **57**, 573–583 (2018).
68. Stang, A. et al. Mobile phone use and risk of uveal melanoma: results of the risk factors for uveal melanoma case-control study. *J. Natl. Cancer Inst.* **101**, 120–123 (2009).
69. Beahm, A. No evidence of Auburn ocular melanoma cluster, Alabama health department says. *AL.com* https://www.al.com/news/2018/10/adph-no-evidence-of-rare-eye-cancer-cluster-in-auburn.html (2018).
70. North Carolina Department of Health and Human Services Division of Public Health. Ocular Melanoma Investigation in Mecklenburg County, North Carolina. https://epi.dph.ncdhhs.gov/oee/docs/OcularMelanomaInvestigationReport_June2015.pdf (2015).
71. Wakamatsu, K., Hu, D.-N., McCormick, S. A. & Ito, S. Characterization of melanin in human iridal and choroidal melanocytes from eyes with various colored irides. *Pigment Cell Melanoma Res.* **21**, 97–105 (2008).
72. Ni-Komatsu, L. & Orlow, S. J. Heterologous expression of tyrosinase recapitulates the misprocessing and mistrafficking in oculocutaneous albinism type 2: effects of altering intracellular pH and pink-eyed dilution gene expression. *Exp. Eye Res.* **82**, 519–528 (2006).
73. Toyofuku, K. et al. The etiology of oculocutaneous albinism (OCA) type II: the pink protein modulates the processing and transport of tyrosinase. *Pigment Cell Res.* **15**, 217–224 (2002).
74. Fuller, B. B., Iman, D. S. & Lunsford, J. B. Comparison of tyrosinase levels in amelanotic and melanotic melanoma cell cultures by a competitive enzyme-linked immunoadsorbent assay and by immunotitration analysis. *J. Cell. Physiol.* **134**, 149–154 (1988).
75. Lee, Y. et al. Characteristics of melanosomes in melanotic and amelanotic melanomas. *J. Hard Tissue Biol.* **13**, 87–90 (2004).
76. Field, M. G. et al. Punctuated evolution of canonical genomic aberrations in uveal melanoma. *Nat. Commun.* **9**, 116 (2018).
77. Moore, A. R. et al. Recurrent activating mutations of G-protein-coupled receptor CYSLTR2 in uveal melanoma. *Nat. Genet.* **48**, 675–680 (2016).
78. Johansson, P. et al. Deep sequencing of uveal melanoma identifies a recurrent mutation in *PLCB4*. *Oncotarget* **7**, 4624–4631 (2016).
79. Yoo, J. H. et al. ARF6 is an actionable node that orchestrates oncogenic GNAQ signaling in uveal melanoma. *Cancer Cell* **29**, 889–904 (2016).
80. Yu, F.-X. et al. Mutant Gq/11 promote uveal melanoma tumorigenesis by activating YAP. *Cancer Cell* **25**, 822–830 (2014).
81. Feng, X. et al. Hippo-independent activation of YAP by the GNAQ uveal melanoma oncogene through a trio-regulated rho GTPase signaling circuitry. *Cancer Cell* **25**, 831–845 (2014).
82. Feng, X. et al. A platform of synthetic lethal gene interaction networks reveals that the GNAQ uveal melanoma oncogene controls the hippo pathway through FAK. *Cancer Cell* **35**, 457–472.e5 (2019).
83. Yasui, F., Miyazu, M., Yoshida, A., Naruse, K. & Takai, A. Examination of signalling pathways involved in muscarinic responses in bovine ciliary muscle using YM-254890, an inhibitor of the Gq/11 protein. *Br. J. Pharmacol.* **154**, 890–900 (2008).
84. Lapadula, D. et al. Effects of oncogenic Gαq and Gα11 inhibition by FR900359 in uveal melanoma. *Mol. Cancer Res.* **17**, 963–973 (2019).
85. Singh, A. D., Kalyani, P. & Topham, A. Estimating the risk of malignant transformation of a choroidal nevus. *Ophthalmology* **112**, 1784–1789 (2005).
86. Carbone, M. et al. BAP1 and cancer. *Nat. Rev. Cancer* **13**, 153–159 (2013).
87. Bononi, A. et al. BAP1 regulates IP3R3-mediated Ca2+ flux to mitochondria suppressing cell transformation. *Nature* **546**, 549–553 (2017).
88. Field, M. G. et al. BAP1 loss is associated with DNA methylomic repatterning in highly aggressive class 2 uveal melanomas. *Clin. Cancer Res.* **25**, 5663–5673 (2019).
89. Scheuermann, J. C. et al. Histone H2A deubiquitinase activity of the Polycomb repressive complex PR-DUB. *Nature* **465**, 243–247 (2010).
90. Wang, L. et al. Resetting the epigenetic balance of Polycomb and COMPASS function at enhancers for cancer therapy. *Nat. Med.* **24**, 758–769 (2018).
91. Campagne, A. et al. BAP1 complex promotes transcription by opposing PRC1-mediated H2A ubiquitylation. *Nat. Commun.* **10**, 348 (2019).
92. Harbour, J. W. et al. Recurrent mutations at codon 625 of the splicing factor SF3B1 in uveal melanoma. *Nat. Genet.* **45**, 133–135 (2013).
93. Darman, R. B. et al. Cancer-associated SF3B1 hotspot mutations induce cryptic 3′ splice site selection through use of a different branch point. *Cell Rep.* **13**, 1033–1045 (2015).
94. Alsafadi, S. et al. Cancer-associated SF3B1 mutations affect alternative splicing by promoting alternative branchpoint usage. *Nat. Commun.* **7**, 10615 (2016).
95. Inoue, D. et al. Spliceosomal disruption of the non-canonical BAF complex in cancer. *Nature* **574**, 432–436 (2019).
96. Johnson, C. P. et al. Systematic genomic and translational efficiency studies of uveal melanoma. *PLoS One* **12**, e0178189 (2017).

97. Shields, C. L. et al. Metastasis of uveal melanoma millimeter-by-millimeter in 8033 consecutive eyes. *Arch. Ophthalmol.* **127**, 989–998 (2009). **An analysis of a very large group of UMs showing that tumour size plays an important part in the development of metastases**.
98. Zimmerman, L. E., McLean, I. W. & Foster, W. D. Does enucleation of the eye containing a malignant melanoma prevent or accelerate the dissemination of tumour cells. *Br. J. Ophthalmol.* **62**, 420–425 (1978).
99. Singh, A. D. The Zimmerman-Mclean-Foster hypothesis: 25 years later. *Br. J. Ophthalmol.* **88**, 962–967 (2004).
100. Yavuzyigitoglu, S. et al. Uveal melanomas with SF3B1 mutations: a distinct subclass associated with late-onset metastases. *Ophthalmology* **123**, 1118–1128 (2016).
101. Szalai, E. et al. Association of uveal melanoma metastatic rate with stochastic mutation rate and type of mutation. *JAMA Ophthalmol.* **136**, 1115–1120 (2018).
102. Koopmans, A. E. et al. Clinical significance of immunohistochemistry for detection of BAP1 mutations in uveal melanoma. *Mod. Pathol.* **27**, 1321–1330 (2014). **This study demonstrated that immunohistochemistry can be used for determining prognosis based on expression of *BAP1***.
103. van Essen, T. H. et al. Prognostic parameters in uveal melanoma and their association with BAP1 expression. *Br. J. Ophthalmol.* **98**, 1738–1743 (2014).
104. Szalai, E., Wells, J. R., Ward, L. & Grossniklaus, H. E. Uveal melanoma nuclear BRCA1-associated protein-1 immunoreactivity is an indicator of metastasis. *Ophthalmology* **125**, 203–209 (2018).
105. Shain, A. H. et al. The genetic evolution of metastatic uveal melanoma. *Nat. Genet.* **51**, 1123–1130 (2019).
106. Rodrigues, M. et al. Evolutionary routes in metastatic uveal melanomas depend on MBD4 alterations. *Clin. Cancer Res.* **25**, 5513–5524 (2019).
107. Piaggio, F. et al. Secondary somatic mutations in G-protein-related pathways and mutation signatures in uveal melanoma. *Cancers* **11**, E1688 (2019).
108. Eide, N. et al. Disseminated tumour cells in bone marrow of patients with uveal melanoma. *Acta Ophthalmol.* **91**, 343–348 (2013).
109. Eide, N. et al. Immunomagnetic detection of micrometastatic cells in bone marrow in uveal melanoma patients. *Acta Ophthalmol.* **87**, 830–836 (2009).
110. Sadegh, L., Chen, P. W., Brown, J. R., Han, Z. & Niederkorn, J. Y. NKT cells act through third party bone marrow-derived cells to suppress NK cell activity in the liver and exacerbate hepatic melanoma metastases: NKT cells and ocular melanoma liver metastases. *Int. J. Cancer* **137**, 1085–1094 (2015).
111. Hendrix, M. J. et al. Regulation of uveal melanoma interconverted phenotype by hepatocyte growth factor/scatter factor (HGF/SF). *Am. J. Pathol.* **152**, 855–863 (1998).
112. Yu, G. et al. Hepatic stellate cells secreted hepatocyte growth factor contributes to the chemoresistance of hepatocellular carcinoma. *PLoS One* **8**, e73312 (2013).
113. Diaz, C. E., Rusciano, D., Dithmar, S. & Grossniklaus, H. E. B16LS9 melanoma cells spread to the liver from the murine ocular posterior compartment (PC). *Curr. Eye Res.* **18**, 125–129 (1999).
114. Li, H., Yang, W., Chen, P. W., Alizadeh, H. & Niederkorn, J. Y. Inhibition of chemokine receptor expression on uveal melanomas by CXCR4 siRNA and its effect on uveal melanoma liver metastases. *Invest. Ophthalmol. Vis. Sci.* **50**, 5522–5528 (2009).
115. Li, H., Alizadeh, H. & Niederkorn, J. Y. Differential expression of chemokine receptors on uveal melanoma cells and their metastases. *Invest. Ophthalmol. Vis. Sci.* **49**, 636–643 (2008).
116. Liepelt, A. & Tacke, F. Stromal cell-derived factor-1 (SDF-1) as a target in liver diseases. *Am. J. Physiol. Gastrointest. Liver Physiol.* **311**, G203–G209 (2016).
117. Zhu, A. et al. Dipyrimidine amines: a novel class of chemokine receptor type 4 antagonists with high specificity. *J. Med. Chem.* **53**, 8556–8568 (2010).
118. Dong, L. et al. Arylsulfonamide 64B inhibits hypoxia/HIF-induced expression of c-Met and CXCR4 and reduces primary tumor growth and metastasis of uveal melanoma. *Clin. Cancer Res.* **25**, 2206–2218 (2019).
119. Grossniklaus, H. E. et al. Metastatic ocular melanoma to the liver exhibits infiltrative and nodular growth patterns. *Hum. Pathol.* **57**, 165–175 (2016).
120. Jones, N. M., Yang, H., Zhang, Q., Morales-Tirado, V. M. & Grossniklaus, H. E. Natural killer cells and pigment epithelial-derived factor control the infiltrative and nodular growth of hepatic metastases in an orthotopic murine model of ocular melanoma. *BMC Cancer* **19**, 484 (2019).
121. Liao, A. et al. Radiologic and histopathologic correlation of different growth patterns of metastatic uveal melanoma to the liver. *Ophthalmology* **125**, 597–605 (2018).
122. Grossniklaus, H. E. Progression of ocular melanoma metastasis to the liver: the 2012 Zimmerman Lecture. *JAMA Ophthalmol.* **131**, 462–469 (2013). **This paper highlights that not all metastases are the same, which may have implications for the treatment of liver metastases**.
123. Eefsen, R. L. et al. Histopathological growth pattern, proteolysis and angiogenesis in chemonaive patients resected for multiple colorectal liver metastases. *J. Oncol.* **2012**, 1–12 (2012).
124. Nwani, N. G. et al. Melanoma cells block PEDF production in fibroblasts to induce the tumor-promoting phenotype of cancer-associated fibroblasts. *Cancer Res.* **76**, 2265–2276 (2016).
125. Niederkorn, J., Streilein, J. W. & Shadduck, J. A. Deviant immune responses to allogeneic tumors injected intracamerally and subcutaneously in mice. *Invest. Ophthalmol. Vis. Sci.* **20**, 355–363 (1981). **The phenomenon of anterior chamber-associated immune deviation is described in this paper**.
126. Schurmans, L. R. et al. Successful immunotherapy of an intraocular tumor in mice. *Cancer Res.* **59**, 5250–5254 (1999).
127. Streilein, J. W. & Niederkorn, J. Y. Induction of anterior chamber-associated immune deviation requires an intact, functional spleen. *J. Exp. Med.* **153**, 1058–1067 (1981).
128. Niederkorn, J. Y. Immune escape mechanisms of intraocular tumors. *Prog. Retin. Eye Res.* **28**, 329–347 (2009).
129. Jiang, L. Q., Jorquera, M. & Streilein, J. W. Subretinal space and vitreous cavity as immunologically privileged sites for retinal allografts. *Invest. Ophthalmol. Vis. Sci.* **34**, 3347–3354 (1993).
130. Knisely, T. L., Luckenbach, M. W., Fischer, B. J. & Niederkorn, J. Y. Destructive and nondestructive patterns of immune rejection of syngeneic intraocular tumors. *J. Immunol.* **138**, 4515–4523 (1987).
131. Thorsson, V. et al. The immune landscape of cancer. *Immunity* **48**, 812–830.e14 (2018).
132. de Waard-Siebinga, I., Hilders, C. G. J. M., Hansen, B. E., van Delft, J. L. & Jager, M. J. HLA expression and tumor-infiltrating immune cells in uveal melanoma. *Graefes Arch. Clin. Exp. Ophthalmol.* **234**, 34–42 (1996).
133. Davidorf, F. H. & Lang, J. R. Lymphocytic infiltration in choroidal melanoma and its prognostic significance. *Trans. Ophthalmol. Soc. UK* **97**, 394–401 (1977).
134. Tobal, K., Deuble, K., McCartney, A. & Lightman, S. Characterization of cellular infiltration in choroidal melanoma. *Melanoma Res.* **3**, 63–65 (1993).
135. Bronkhorst, I. H. G. et al. Different subsets of tumor-infiltrating lymphocytes correlate with macrophage influx and monosomy 3 in uveal melanoma. *Invest. Ophthalmol. Vis. Sci.* **53**, 5370–5378 (2012).
136. Lagouros, E. et al. Infiltrative T regulatory cells in enucleated uveal melanomas. *Trans. Am. Ophthalmol. Soc.* **107**, 223–228 (2009).
137. Gezgin, G. et al. Genetic evolution of uveal melanoma guides the development of an inflammatory microenvironment. *Cancer Immunol. Immunother.* **66**, 903–912 (2017).
138. Figueiredo, C. R. et al. Loss of BAP1 expression is associated with an immunosuppressive microenvironment in uveal melanoma, with implications for immunotherapy development. *J. Pathol.* **250**, 420–439 (2020).
139. McGranahan, N. et al. Clonal neoantigens elicit T cell immunoreactivity and sensitivity to immune checkpoint blockade. *Science* **351**, 1463–1469 (2016).
140. Colli, L. M. et al. Burden of nonsynonymous mutations among TCGA cancers and candidate immune checkpoint inhibitor responses. *Cancer Res.* **76**, 3767–3772 (2016).
141. van der Pol, J. P. et al. Heterogeneous expression of melanoma-associated antigens in uveal melanomas. *Curr. Eye Res.* **6**, 757–765 (1987).
142. de Vries, T. J., Trancikova, D., Ruiter, D. J. & van Muijen, G. N. High expression of immunotherapy candidate proteins gp100, MART-1, tyrosinase and TRP-1 in uveal melanoma. *Br. J. Cancer* **78**, 1156–1161 (1998).
143. Mulcahy, K. A. et al. Infrequent expression of the MAGE gene family in uveal melanomas. *Int. J. Cancer* **66**, 738–742 (1996).
144. Field, M. G. et al. PRAME as an independent biomarker for metastasis in uveal melanoma. *Clin. Cancer Res.* **22**, 1234–1242 (2016).
145. Gezgin, G. et al. PRAME as a potential target for immunotherapy in metastatic uveal melanoma. *JAMA Ophthalmol.* **135**, 541–549 (2017).
146. Garrido, F. & Algarra, I. MHC antigens and tumor escape from immune surveillance. *Adv. Cancer Res.* **83**, 117–158 (2001).
147. Anastassiou, G., Rebmann, V., Wagner, S., Bornfeld, N. & Grosse-Wilde, H. Expression of classic and nonclassic HLA class I antigens in uveal melanoma. *Invest. Ophthalmol. Vis. Sci.* **44**, 2016–2019 (2003).
148. Blom, D. J. et al. Human leukocyte antigen class I expression. Marker of poor prognosis in uveal melanoma. *Invest. Ophthalmol. Vis. Sci.* **38**, 1865–1872 (1997).
149. Ericsson, C. et al. Association of HLA class I and class II antigen expression and mortality in uveal melanoma. *Invest. Ophthalmol. Vis. Sci.* **42**, 2153–2156 (2001).
150. Dithmar, S., Crowder, J., Jager, M. J., Vigniswaran, N. & Grossniklaus, H. E. HLA class I antigen expression correlates with histological cell type in uveal melanoma. *Ophthalmology* **99**, 625–628 (2002).
151. Jager, M. J., Hurks, H. M., Levitskaya, J. & Kiessling, R. HLA expression in uveal melanoma: there is no rule without some exception. *Hum. Immunol.* **63**, 444–451 (2002).
152. Dithmar, S., Rusciano, D., Armstrong, C. A., Lynn, M. J. & Grossniklaus, H. E. Depletion of NK cell activity results in growth of hepatic micrometastases in a murine ocular melanoma model. *Curr. Eye Res.* **19**, 426–431 (1999).
153. Ma, D., Luyten, G. P., Luider, T. M. & Niederkorn, J. Y. Relationship between natural killer cell susceptibility and metastasis of human uveal melanoma cells in a murine model. *Invest. Ophthalmol. Vis. Sci.* **36**, 435–441 (1995).
154. Souri, Z., Wierenga, A. P. A., Mulder, A., Jochemsen, A. G. & Jager, M. J. HLA expression in uveal melanoma: an indicator of malignancy and a modifiable immunological target. *Cancers* **11**, 1132 (2019).
155. van Essen, T. H. et al. Upregulation of HLA expression in primary uveal melanoma by infiltrating leukocytes. *PLoS One* **11**, e0164292 (2016).
156. de Waard-Siebinga, I., Creyghton, W. M., Kool, J. & Jager, M. J. Effects of interferon alfa and gamma on human uveal melanoma cells in vitro. *Br. J. Ophthalmol.* **79**, 847–855 (1995).
157. Mäkitie, T., Summanen, P., Tarkkanen, A. & Kivelä, T. Microvascular density in predicting survival of patients with choroidal and ciliary body melanoma. *Invest. Ophthalmol. Vis. Sci.* **40**, 2471–2480 (1999).
158. Mäkitie, T., Summanen, P., Tarkkanen, A. & Kivelä, T. Tumor-infiltrating macrophages (CD68+ cells) and prognosis in malignant uveal melanoma. *Invest. Ophthalmol. Vis. Sci.* **42**, 1414–1421 (2001). **This study found that the presence of tumour-infiltrating macrophages is associated with poor prognosis**.
159. Bronkhorst, I. H. G. et al. Detection of M2-macrophages in uveal melanoma and relation with survival. *Invest. Ophthalmol. Vis. Sci.* **52**, 643–650 (2011). **This study demonstrated that in UM, infiltrating macrophages are proangiogenic, explaining their association with poor prognosis; proangiogenic macrophages help the formation of blood vessels, which are essential for metastasis**.
160. Brouwer, N. J. et al. Tumour angiogenesis in uveal melanoma is related to genetic evolution. *Cancers* **11**, E979 (2019).
161. McKenna, K. C. et al. Activated CD11b+ CD15+ granulocytes increase in the blood of patients with uveal melanoma. *Invest. Ophthalmol. Vis. Sci.* **50**, 4295–4303 (2009).
162. Carlring, J., Shaif-Muthana, M., Sisley, K., Rennie, I. G. & Murray, A. K. Apoptotic cell death in conjunction with CD80 costimulation confers uveal melanoma cells with the ability to induce immune responses. *Immunology* **109**, 41–48 (2003).
163. Bosch, J. J. et al. MHC class II-transduced tumor cells originating in the immune-privileged eye prime and boost CD4(+) T lymphocytes that cross-react with primary and metastatic uveal melanoma cells. *Cancer Res.* **67**, 4499–4506 (2007).
164. Verbik, D. J., Murray, T. G., Tran, J. M. & Ksander, B. R. Melanomas that develop within the eye inhibit lymphocyte proliferation. *Int. J. Cancer* **73**, 470–478 (1997).
165. Wierenga, A. P. A., Cao, J., Luyten, G. P. M. & Jager, M. J. Immune checkpoint inhibitors in uveal

and conjunctival melanoma. *Int. Ophthalmol. Clin.* **59**, 53–63 (2019).
166. Durante, M. A. et al. Single-cell analysis reveals new evolutionary complexity in uveal melanoma. *Nat. Commun.* **11**, 496 (2020).
167. Yang, W. et al. PD-L1 expression on human ocular cells and its possible role in regulating immune-mediated ocular inflammation. *Invest. Ophthalmol. Vis. Sci.* **50**, 273–280 (2009).
168. Hallermalm, K. et al. Modulation of the tumor cell phenotype by IFN-γ results in resistance of uveal melanoma cells to granule-mediated lysis by cytotoxic lymphocytes. *J. Immunol.* **180**, 3766–3774 (2008).
169. Chen, P. W. et al. Uveal melanoma expression of indoleamine 2,3-deoxygenase: establishment of an immune privileged environment by tryptophan depletion. *Exp. Eye Res.* **85**, 617–625 (2007).
170. Felberg, N. T., Donoso, L. A. & Federman, J. L. Tumor-associated antibodies in the serum of patients with ocular melanoma. IV. Correction for smooth muscle antibodies. *Ophthalmol.* **87**, 529–533 (1980).
171. Rahi, A. H. Autoimmune reactions in uveal melanoma. *Br. J. Ophthalmol.* **55**, 793–807 (1971).
172. Goslings, W. R. et al. Membrane-bound regulators of complement activation in uveal melanomas. CD46, CD55, and CD59 in uveal melanomas. *Invest. Ophthalmol. Vis. Sci.* **37**, 1884–1891 (1996).
173. Kan-Mitchell, J. et al. Lymphocytes cytotoxic to uveal and skin melanoma cells from peripheral blood of ocular melanoma patients. *Cancer Immunol. Immunother.* **33**, 333–340 (1991).
174. Ksander, B. R. et al. Uveal melanomas contain antigenically specific and non-specific infiltrating lymphocytes. *Curr. Eye Res.* **17**, 165–173 (1998).
175. Ksander, B. R., Rubsamen, P. E., Olsen, K. R., Cousins, S. W. & Streilein, J. W. Studies of tumor-infiltrating lymphocytes from a human choroidal melanoma. *Invest. Ophthalmol. Vis. Sci.* **32**, 3198–3208 (1991).
176. Rothermel, L. D. et al. Identification of an immunogenic subset of metastatic uveal melanoma. *Clin. Cancer Res.* **22**, 2237–2249 (2016).
177. Chandran, S. S. et al. Treatment of metastatic uveal melanoma with adoptive transfer of tumour-infiltrating lymphocytes: a single-centre, two-stage, single-arm, phase 2 study. *Lancet Oncol.* **18**, 792–802 (2017).
178. Krishna, Y., McCarthy, C., Kalirai, H. & Coupland, S. E. Inflammatory cell infiltrates in advanced metastatic uveal melanoma. *Hum. Pathol.* **66**, 159–166 (2017).
179. Foster, A. D., Sivarapatna, A. & Gress, R. E. The aging immune system and its relationship with cancer. *Aging Health* **7**, 707–718 (2011).
180. Sandinha, T., Hebbar, G., Kenawy, N., Hope-Stone, L. & Damato, B. A nurse-led ocular oncology clinic in Liverpool: results of a 6-month trial. *Eye* **26**, 937–943 (2012).
181. Smith, J. R. et al. Proceedings of the Association for Research in Vision and Ophthalmology and Champalimaud Foundation Ocular Oncogenesis and Oncology Conference. *Transl. Vis. Sci. Technol.* **8**, 9 (2019).
182. Shields, J. A. & Shields, C. L. Management of posterior uveal melanoma: past, present, and future: the 2014 Charles L. Schepens Lecture. *Ophthalmology* **122**, 414–428 (2015).
183. Kivelä, T. Diagnosis of uveal melanoma. *Dev. Ophthalmol.* **49**, 1–15 (2012).
184. Dogrusöz, M., Jager, M. J. & Damato, B. Uveal melanoma treatment and prognostication. *Asia-Pac. J. Ophthalmol.* **6**, 186–196 (2017).
185. Shields, C. L., Manalac, J., Das, C., Ferguson, K. & Shields, J. A. Choroidal melanoma: clinical features, classification, and top 10 pseudomelanomas. *Curr. Opin. Ophthalmol.* **25**, 177–185 (2014).
186. Shields, C. L. et al. Clinical survey of 3680 iris tumors based on patient age at presentation. *Ophthalmology* **119**, 407–414 (2012).
187. Shields, C. L., Kaliki, S., Furuta, M., Mashayekhi, A. & Shields, J. A. Clinical spectrum and prognosis of uveal melanoma based on age at presentation in 8,033 cases. *Retina* **32**, 1363–1372 (2012).
188. Shields, C. L. et al. Visual outcome and millimeter incremental risk of metastasis in 1780 patients with small choroidal melanoma managed by plaque radiotherapy. *JAMA Ophthalmol.* **136**, 1325–1333 (2018).
189. Shields, C. L. et al. Large uveal melanoma (≥10 mm thickness): clinical features and millimeter-by-millimeter risk of metastasis in 1311 cases. The 2018 Albert E. Finley Lecture. *Retina* **38**, 2010–2022 (2018).
190. Shields, C. L. et al. Choroidal nevus imaging features in 3,806 cases and risk factors for transformation into melanoma in 2,355 cases: the 2020 Taylor R. Smith and Victor T. Curtin Lecture. *Retina* **39**, 1840–1851 (2018).
This paper defines the characteristics of naevi that transform into UM.
191. Coleman, D. J. et al. High-resolution ultrasonic imaging of the posterior segment. *Ophthalmology* **111**, 1344–1351 (2004).
192. Lois, N. Cavitary melanoma of the ciliary body A study of eight cases. *Ophthalmology* **105**, 1091–1098 (1998).
193. Nordlund, J. R., Robertson, D. M. & Herman, D. C. Ultrasound biomicroscopy in management of malignant iris melanoma. *Arch. Ophthalmol.* **121**, 725–727 (2003).
194. Bianciotto, C. et al. Assessment of anterior segment tumors with ultrasound biomicroscopy versus anterior segment optical coherence tomography in 200 cases. *Ophthalmology* **118**, 1297–1302 (2011).
195. Damato, B. E. Tumour fluorescence and tumour-associated fluorescence of choroidal melanomas. *Eye* **6**, 587–593 (1992).
196. Damato, B. E. & Foulds, W. S. Tumour-associated retinal pigment epitheliopathy. *Eye* **4**, 382–387 (1990).
197. Shields, C. L., Shields, J. A. & De Potter, P. Patterns of indocyanine green videoangiography of choroidal tumours. *Br. J. Ophthalmol.* **79**, 237–245 (1995).
198. Shields, C. L. et al. Autofluorescence of choroidal melanoma in 51 cases. *Br. J. Ophthalmol.* **92**, 617–622 (2008).
199. Shields, C. L. et al. Autofluorescence of choroidal nevus in 64 cases. *Retina* **28**, 1035–1043 (2008).
200. Shields, C. L., Bianciotto, C., Pirondini, C. & Shields, J. A. Autofluorescence of intraocular tumors. *Invest. Ophthalmol. Vis. Sci.* **49**, 5689–5689 (2008).
201. Bindewald-Wittich, A., Swenshon, T., Carasco, E., Dreyhaupt, J. & Willerding, G. D. Blue-light fundus autofluorescence imaging following ruthenium-106 brachytherapy for choroidal melanoma. *Ophthalmologica* https://doi.org/10.1159/000504715 (2020).
202. Muscat, S. Secondary retinal changes associated with choroidal naevi and melanomas documented by optical coherence tomography. *Br. J. Ophthalmol.* **88**, 120–124 (2004).
203. Singh, A. D., Belfort, R. N., Sayanagi, K. & Kaiser, P. K. Fourier domain optical coherence tomographic and auto-fluorescence findings in indeterminate choroidal melanocytic lesions. *Br. J. Ophthalmol.* **94**, 474–478 (2010).
204. Shah, S. U. et al. Enhanced depth imaging optical coherence tomography of choroidal nevus in 104 cases. *Ophthalmol.* **119**, 1066–1072 (2012).
205. Shields, C. L., Pellegrini, M., Ferenczy, S. R. & Shields, J. A. Enhanced depth imaging optical coherence tomography of intraocular tumors: from placid to seasick to rock and rolling topography — the 2013 Francesco Orzalesi Lecture. *Retina* **34**, 1495–1512 (2014).
206. Damato, B. E., Heimann, H., Kalirai, H. & Coupland, S. E. Age, survival predictors, and metastatic death in patients with choroidal melanoma: tentative evidence of a therapeutic effect on survival. *JAMA Ophthalmol.* **132**, 605–613 (2014).
207. Shields, C., Manalac, J., Saktanasate, J., Shields, J. & Das, C. Review of spectral domain enhanced depth imaging optical coherence tomography of tumors of the choroid. *Indian. J. Ophthalmol.* **63**, 117–121 (2015).
208. Valverde-Megías, A., Say, E. A. T., Ferenczy, S. R. & Shields, C. L. Differential macular features on optical coherence tomography angiography in eyes with choroidal nevus and melanoma. *Retina* **37**, 731–740 (2017).
209. Shields, C. L. et al. Optical coherence tomography angiography of the macula after plaque radiotherapy of choroidal melanoma: comparison of irradiated versus nonirradiated eyes in 65 patients. *Retina* **36**, 1493–1505 (2016).
210. Brouwer, N. J. et al. Retinal oximetry is altered in eyes with choroidal melanoma but not in eyes with choroidal nevi. *Retina* https://doi.org/10.1097/IAE.0000000000002719 (2019).
211. Beenakker, J.-W. M. et al. Clinical evaluation of ultra-high-field MRI for three-dimensional visualisation of tumour size in uveal melanoma patients, with direct relevance to treatment planning. *MAGMA* **29**, 571–577 (2016).
212. Tartaglione, T. et al. Uveal melanoma: evaluation of extrascleral extension using thin-section MR of the eye with surface coils. *Radiol. Med.* **119**, 775–783 (2014).
213. Ferreira, T. et al. MRI of uveal melanoma. *Cancers* **11**, E377 (2019).
214. Shields, J. A., Shields, C. L., Ehya, H., Eagle, R. C. & De Potter, P. Fine-needle aspiration biopsy of suspected intraocular tumors. The 1992 Urwick Lecture. *Ophthalmology* **100**, 1677–1684 (1993).
215. Midena, E. et al. In vivo detection of monosomy 3 in eyes with medium-sized uveal melanoma using transscleral fine needle aspiration biopsy. *Eur. J. Ophthalmol.* **16**, 422–425 (2006).
216. Shields, C. L. et al. Personalized prognosis of uveal melanoma based on cytogenetic profile in 1059 patients over an 8-year period. *Ophthalmology* **124**, 1523–1531 (2017).
217. Shields, C. L. et al. Prognosis of uveal melanoma in 500 cases using genetic testing of fine-needle aspiration biopsy specimens. *Ophthalmology* **118**, 396–401 (2011).
218. Shields, C. L. et al. Cytogenetic abnormalities in uveal melanoma based on tumor features and size in 1059 patients. *Ophthalmology* **124**, 609–618 (2017).
219. Scholes, A. G. M. et al. Monosomy 3 in uveal melanoma: correlation with clinical and histologic predictors of survival. *Invest. Ophthalmol. Vis. Sci.* **44**, 1008–1011 (2003).
220. Callender, G. R. Malignant melanotic tumors of the eye: a study of histologic types in 111 cases. *Trans. Am. Acad. Ophthalmol. Otolaryngol.* **36**, 131–140 (1931).
221. McLean, I. W., Foster, W. D., Zimmerman, L. E. & Gamel, J. W. Modifications of Callender's classification of uveal melanoma at the Armed Forces Institute of Pathology. *Am. J. Ophthalmol.* **96**, 502–509 (1983).
222. Fernandes, B. F. et al. Immunohistochemical expression of melan-A and tyrosinase in uveal melanoma. *J. Carcinog.* **6**, 6 (2007).
223. O'Reilly, F. M. et al. Microphthalmia transcription factor immunohistochemistry: a useful diagnostic marker in the diagnosis and detection of cutaneous melanoma, sentinel lymph node metastases, and extracutaneous melanocytic neoplasms. *J. Am. Acad. Dermatol.* **45**, 414–419 (2001).
224. Mouriaux, F. et al. Expression of the c-kit receptor in choroidal melanomas. *Melanoma Res.* **13**, 161–166 (2003).
225. Amin, M. B. et al. The eighth edition AJCC Cancer Staging Manual: continuing to build a bridge from a population-based to a more 'personalized' approach to cancer staging. *CA. Cancer J. Clin.* **67**, 93–99 (2017).
226. Folberg, R. et al. The prognostic value of tumor blood vessel morphology in primary uveal melanoma. *Ophthalmology* **100**, 1389–1398 (1993).
227. Shields, J. A. & Shields, C. L. *Intraocular Tumors: An Atlas and Textbook* 3rd edn (Wolters Kluwer, 2015).
228. Damato, B. Progress in the management of patients with uveal melanoma. The 2012 Ashton Lecture. *Eye* **26**, 1157–1172 (2012).
229. Manschot, W. A. & Van Strik, R. Is irradiation a justifiable treatment of choroidal melanoma? Analysis of published results. *Br. J. Ophthalmol.* **71**, 348–352 (1987).
230. Collaborative Ocular Melanoma Study Group. The COMS randomized trial of iodine 125 brachytherapy for choroidal melanoma, III: initial mortality findings. COMS Report No. 18. *Arch. Ophthalmol.* **119**, 969–982 (2001).
231. Collaborative Ocular Melanoma Study Group. The COMS randomized trial of iodine 125 brachytherapy for choroidal melanoma: V. Twelve-year mortality rates and prognostic factors: COMS report No. 28. *Arch. Ophthalmol.* **124**, 1684–1693 (2006).
232. Collaborative Ocular Melanoma Study Group. The Collaborative Ocular Melanoma Study (COMS) randomized trial of pre-enucleation radiation of large choroidal melanoma: IV. Ten-year mortality findings and prognostic factors. COMS report number 24. *Am. J. Ophthalmol.* **138**, 936–951 (2004).
233. Sagoo, M. S. et al. Plaque radiotherapy for juxtapapillary choroidal melanoma: tumor control in 650 consecutive cases. *Ophthalmology* **118**, 402–407 (2011).
234. Shields, C. L. et al. Iris melanoma management with iodine-125 plaque radiotherapy in 144 patients: impact of melanoma-related glaucoma on outcomes. *Ophthalmology* **120**, 55–61 (2013).
235. Gündüz, K., Shields, C. L., Shields, J. A., Cater, J. & Brady, L. Plaque radiotherapy for management of ciliary body and choroidal melanoma with extraocular extension. *Am. J. Ophthalmol.* **130**, 97–102 (2000).
236. Shah, S. U. et al. Intravitreal bevacizumab at 4-month intervals for prevention of macular edema after plaque

radiotherapy of uveal melanoma. *Ophthalmology* **121**, 269–275 (2014).
237. Gragoudas, E. S., Lane, A. M., Munzenrider, J., Egan, K. M. & Li, W. Long-term risk of local failure after proton therapy for choroidal/ciliary body melanoma. *Trans. Am. Ophthalmol. Soc.* **100**, 43–48 (2002).
238. Damato, B. in *Retinal Vascular Disease* (eds Joussen, A. M., Gardner, T. W., Kirchhof, B. & Ryan, S. J.) 582–591 (Springer, 2007).
239. Shields, C. L., Shields, J. A., Gündüz, K., Freire, J. E. & Mercado, G. Radiation therapy for uveal malignant melanoma. *Ophthalmic Surg. Lasers* **29**, 397–409 (1998).
240. Lommatzsch, P. & Vollmar, R. A new way in the conservative therapy of intraocular tumors by means of beta-irradiation (ruthenium 106) with preservation of vision [German]. *Klin. Monatsbl. Augenheilkd.* **148**, 682–699 (1966).
241. Horgan, N. et al. Periocular triamcinolone for prevention of macular edema after plaque radiotherapy of uveal melanoma: a randomized controlled trial. *Ophthalmology* **116**, 1383–1390 (2009).
242. Shields, C. L. et al. Plaque radiotherapy for uveal melanoma: long-term visual outcome in 1106 consecutive patients. *Arch. Ophthalmol.* **118**, 1219–1228 (2000).
243. Collaborative Ocular Melanoma Study Group. Collaborative ocular melanoma study (COMS) randomized trial of I-125 brachytherapy for medium choroidal melanoma. I. Visual acuity after 3 years COMS report no. 16. *Ophthalmology* **108**, 348–366 (2001).
244. Gragoudas, E. S. et al. Proton beam irradiation. An alternative to enucleation for intraocular melanomas. *Ophthalmology* **87**, 571–581 (1980).
245. Gragoudas, E. S. Proton beam irradiation of uveal melanomas: the first 30 years. The Weisenfeld Lecture. *Invest. Ophthalmol. Vis. Sci.* **47**, 4666–4673 (2006).
246. Damato, B. et al. Proton beam radiotherapy of iris melanoma. *Int. J. Radiat. Oncol. Biol. Phys.* **63**, 109–115 (2005).
247. Akbaba, S. et al. Linear accelerator-based stereotactic fractionated photon radiotherapy as an eye-conserving treatment for uveal melanoma. *Radiat. Oncol.* **13**, 140 (2018).
248. Siedlecki, J. et al. Incidence of secondary glaucoma after treatment of uveal melanoma with robotic radiosurgery versus brachytherapy. *Acta Ophthalmol.* **95**, e734–e739 (2017).
249. Oosterhuis, J. A., Journée-de Korver, H. G. & Keunen, J. E. Transpupillary thermotherapy: results in 50 patients with choroidal melanoma. *Arch. Ophthalmol.* **116**, 157–162 (1998).
250. Shields, C. L., Shields, J. A., Perez, N., Singh, A. D. & Cater, J. Primary transpupillary thermotherapy for small choroidal melanoma in 256 consecutive cases: outcomes and limitations. *Ophthalmology* **109**, 225–234 (2002).
251. Mashayekhi, A. et al. Primary transpupillary thermotherapy for choroidal melanoma in 391 cases: importance of risk factors in tumor control. *Ophthalmology* **122**, 600–609 (2015).
252. Marinkovic, M. et al. Ruthenium-106 brachytherapy for choroidal melanoma without transpupillary thermotherapy: similar efficacy with improved visual outcome. *Eur. J. Cancer* **68**, 106–113 (2016).
253. Blasi, M. A. et al. Brachytherapy alone or with neoadjuvant photodynamic therapy for amelanotic choroidal melanoma: functional outcomes and local tumor control. *Retina* **36**, 2205–2212 (2016).
254. Campbell, W. G. & Pejnovic, T. M. Treatment of amelanotic choroidal melanoma with photodynamic therapy. *Retina* **32**, 1356–1362 (2012).
255. Turkoglu, E. B., Pointdujour-Lim, R., Mashayekhi, A. & Shields, C. L. Photodynamic therapy as primary treatment for small choroidal melanoma. *Retina* **39**, 1319–1325 (2018).
256. Rundle, P. Treatment of posterior uveal melanoma with multi-dose photodynamic therapy. *Br. J. Ophthalmol.* **98**, 494–497 (2014).
257. Shields, C. L., Lim, L.-A. S., Dalvin, L. A. & Shields, J. A. Small choroidal melanoma: detection with multimodal imaging and management with plaque radiotherapy or AU-011 nanoparticle therapy. *Curr. Opin. Ophthalmol.* **30**, 206–214 (2019).
258. Kines, R. C. et al. An infrared dye-conjugated virus-like particle for the treatment of primary uveal melanoma. *Mol. Cancer Ther.* **17**, 565–574 (2018).
259. Damato, B. E., Afshar, R., Stewart, J., Groenwald, C. & Foulds, W. S. in *Retina* Vol. 3 (ed. Ryan, S. J.) 2298–2306 (Elsevier, 2013).
260. Shields, J. A., Shields, C. L., Shah, P. & Sivalingam, V. Partial lamellar sclerouvectomy for ciliary body and choroidal tumors. *Ophthalmology* **98**, 971–983 (1991).
261. Damato, B. The role of eyewall resection in uveal melanoma management. *Int. Ophthalmol. Clin.* **46**, 81–93 (2006).
262. Kivelä, T., Puusaari, I. & Damato, B. Transscleral resection versus iodine brachytherapy for choroidal malignant melanomas 6 millimeters or more in thickness. *Ophthalmology* **110**, 2235–2244 (2003).
263. Bechrakis, N. E. & Foerster, M. H. Neoadjuvant proton beam radiotherapy combined with subsequent endoresection of choroidal melanomas. *Int. Ophthalmol. Clin.* **46**, 95–107 (2006).
264. Konstantinidis, L., Groenewald, C., Coupland, S. E. & Damato, B. Long-term outcome of primary endoresection of choroidal melanoma. *Br. J. Ophthalmol.* **98**, 82–85 (2014).
265. Barker, C. A. & Salama, A. K. New NCCN guidelines for uveal melanoma and treatment of recurrent or progressive distant metastatic melanoma. *J. Natl Compr. Cancer Netw.* **16**, 646–650 (2018).
266. Bellerive, C. et al. Local failure after episcleral brachytherapy for posterior uveal melanoma: patterns, risk factors, and management. *Am. J. Ophthalmol.* **177**, 9–16 (2017).
267. AJCC Ophthalmic Oncology Task Force. International validation of the American Joint Committee on Cancer's 7th Edition Classification of Uveal Melanoma. *JAMA Ophthalmol.* **133**, 376–383 (2015).
268. Gündüz, K. et al. Radiation complications and tumor control after plaque radiotherapy of choroidal melanoma with macular involvement. *Am. J. Ophthalmol.* **127**, 579–589 (1999).
269. Wisely, C. E. et al. Long-term visual acuity outcomes in patients with uveal melanoma treated with 125I episcleral OSU-Nag plaque brachytherapy. *Brachytherapy* **15**, 12–22 (2016).
270. Horgan, N. et al. Periocular triamcinolone for prevention of macular edema after iodine 125 plaque radiotherapy of uveal melanoma. *Retina* **28**, 987–995 (2008).
271. Materin, M. A., Bianciotto, C. G., Wu, C. & Shields, C. L. Sector laser photocoagulation for the prevention of macular edema after plaque radiotherapy for uveal melanoma: a pilot study. *Retina* **32**, 1601–1607 (2012).
272. DeParis, S. W. et al. External validation of the Liverpool uveal melanoma prognosticator online. *Invest. Ophthalmol. Vis. Sci.* **57**, 6116–6122 (2016).
273. Valsecchi, M. E. et al. Adjuvant sunitinib in high-risk patients with uveal melanoma: comparison with institutional controls. *Ophthalmology* **125**, 210–217 (2018).
274. McLean, M. J., Foster, W. D. & Zimmerman, L. E. Prognostic factors in small malignant melanomas of choroid and ciliary body. *Arch. Ophthalmol.* **95**, 48–58 (1977).
275. de la Cruz, P. O., Specht, C. S. & McLean, I. W. Lymphocytic infiltration in uveal malignant melanoma. *Cancer* **65**, 112–115 (1990).
276. Prescher, G., Bornfeld, N., Horsthemke, B. & Becher, R. Chromosomal aberrations defining uveal melanoma of poor prognosis. *Lancet* **339**, 691–692 (1992).
277. Horsman, D. E., Sroka, H., Rootman, J. & White, V. A. Monosomy 3 and isochromosome 8q in a uveal melanoma. *Cancer Genet. Cytogenet.* **45**, 249–253 (1990).
This paper provides the first description of the presence of specific chromosomal aberrations in primary UM.
278. Sisley, K. et al. Abnormalities of chromosomes 3 and 8 in posterior uveal melanoma correlate with prognosis. *Genes. Chromosomes Cancer* **19**, 22–28 (1997).
279. White, V. A., Chambers, J. D., Courtright, P. D., Chang, W. Y. & Horsman, D. E. Correlation of cytogenetic abnormalities with the outcome of patients with uveal melanoma. *Cancer* **83**, 354–359 (1998).
280. Damato, B. et al. Cytogenetics of uveal melanoma: a 7-year clinical experience. *Ophthalmology* **114**, 1925–1931 (2007).
281. Damato, B., Eleuteri, A., Taktak, A. F. G. & Coupland, S. E. Estimating prognosis for survival after treatment of choroidal melanoma. *Prog. Retin. Eye Res.* **30**, 285–295 (2011).
282. Cassoux, N. et al. Genome-wide profiling is a clinically relevant and affordable prognostic test in posterior uveal melanoma. *Br. J. Ophthalmol.* **98**, 769–774 (2014).
283. Tschentscher, F. et al. Tumor classification based on gene expression profiling shows that uveal melanomas with and without monosomy 3 represent two distinct entities. *Cancer Res.* **63**, 2578–2584 (2003).
284. Dogrusöz, M. & Jager, M. J. Genetic prognostication in uveal melanoma. *Acta Ophthalmol.* **96**, 331–347 (2018).
285. Dogrusöz, M. et al. The prognostic value of AJCC staging in uveal melanoma is enhanced by adding chromosome 3 and 8q status. *Invest. Ophthalmol. Vis. Sci.* **58**, 833 (2017).
286. Bagger, M. et al. The prognostic effect of American Joint Committee on Cancer staging and genetic status in patients with choroidal and ciliary body melanoma. *Invest. Ophthalmol. Vis. Sci.* **56**, 438–444 (2014).
287. Onken, M. D. et al. Collaborative Ocular Oncology Group report number 1: prospective validation of a multi-gene prognostic assay in uveal melanoma. *Ophthalmology* **119**, 1596–1603 (2012).
288. Eleuteri, A., Damato, B., Coupland, S. E. & Taktak, A. F. G. Enhancing survival prognostication in patients with choroidal melanoma by integrating pathologic, clinical and genetic predictors of metastasis. *Int. J. Biomed. Eng. Technol.* **8**, 18–35 (2012).
289. Vaquero-Garcia, J. et al. PRiMeUM: a model for predicting risk of metastasis in uveal melanoma. *Invest. Ophthalmol. Vis. Sci.* **58**, 4096–4105 (2017).
290. Nathan, P. et al. Uveal melanoma UK national guidelines. *Eur. J. Cancer* **51**, 2404–2412 (2015).
291. Ritsma, L. et al. Intravital microscopy through an abdominal imaging window reveals a pre-micrometastasis stage during liver metastasis. *Sci. Transl. Med.* **4**, 158ra145 (2012).
292. Richtig, E. et al. Safety and efficacy of interferon alfa-2b in the adjuvant treatment of uveal melanoma [German]. *Ophthalmologe* **103**, 506–511 (2006).
293. Lane, A. M. et al. Adjuvant interferon therapy for patients with uveal melanoma at high risk of metastasis. *Ophthalmology* **116**, 2206–2212 (2009).
294. McLean, I. W. et al. A randomized study of methanol-extraction residue of bacille Calmette-Guerin as postsurgical adjuvant therapy of uveal melanoma. *Am. J. Ophthalmol.* **110**, 522–526 (1990).
295. Desjardins, L. et al. Etude randomisée de chimiothérapie adjuvante par le Déticène dans le mélanome choroïdien [French]. *Ophtalmologie* **12**, 168–173 (1998).
296. Desjardins, L. et al. Adjuvant intravenous therapy by fotemustine in uveal melanoma: a randomised study [abstract]. *Acta Ophthalmol.* https://doi.org/10.1111/j.1755-3768.2011.4362.x (2011).
297. Leyvraz, S. et al. Hepatic intra-arterial versus intravenous fotemustine in patients with liver metastases from uveal melanoma (EORTC 18021): a multicentric randomized trial. *Ann. Oncol.* **25**, 742–746 (2014).
298. Hughes, M. S. et al. Results of a randomized controlled multicenter phase III trial of percutaneous hepatic perfusion compared with best available care for patients with melanoma liver metastases. *Ann. Surg. Oncol.* **23**, 1309–1319 (2016).
299. Bhatia, S. et al. Phase II trial of sorafenib in combination with carboplatin and paclitaxel in patients with metastatic uveal melanoma: SWOG S0512. *PLoS One* **7**, e48787 (2012).
300. Homsi, J. et al. Phase 2 open-label study of weekly docosahexaenoic acid-paclitaxel in patients with metastatic uveal melanoma. *Melanoma Res.* **20**, 507–510 (2010).
301. O'Neill, P. A., Butt, M., Eswar, C. V., Gillis, P. & Marshall, E. A prospective single arm phase II study of dacarbazine and treosulfan as first-line therapy in metastatic uveal melanoma. *Melanoma Res.* **16**, 245–248 (2006).
302. Schmittel, A. et al. Phase II trial of cisplatin, gemcitabine and treosulfan in patients with metastatic uveal melanoma. *Melanoma Res.* **15**, 205–207 (2005).
303. Schmittel, A. et al. A two-cohort phase II clinical trial of gemcitabine plus treosulfan in patients with metastatic uveal melanoma. *Melanoma Res.* **15**, 447–451 (2005).
304. Schmidt-Hieber, M., Schmittel, A., Thiel, E. & Keilholz, U. A phase II study of bendamustine chemotherapy as second-line treatment in metastatic uveal melanoma. *Melanoma Res.* **14**, 439–442 (2004).
305. Bedikian, A. Y., Papadopoulos, N., Plager, C., Eton, O. & Ring, S. Phase II evaluation of temozolomide in metastatic choroidal melanoma. *Melanoma Res.* **13**, 303–306 (2003).
306. Kivelä, T. et al. Bleomycin, vincristine, lomustine and dacarbazine (BOLD) in combination with recombinant interferon alpha-2b for metastatic uveal melanoma. *Eur. J. Cancer* **39**, 1115–1120 (2003).
307. Carvajal, R. D. et al. Effect of selumetinib vs chemotherapy on progression-free survival in uveal

melanoma: a randomized clinical trial. *JAMA* **311**, 2397–2405 (2014).
308. Carvajal, R. D. et al. Selumetinib in combination with dacarbazine in patients with metastatic uveal melanoma: a phase III, multicenter, randomized trial (SUMIT). *J. Clin. Oncol.* **36**, 1232–1239 (2018).
309. Piperno-Neumann, S. et al. Phase I dose-escalation study of the protein kinase C (PKC) inhibitor AEB071 in patients with metastatic uveal melanoma [abstract]. *J. Clin. Oncol.* **32** (Suppl. 15), 9030 (2014).
310. Kapiteijn, E. et al. A phase I trial of LXS196, a novel PKC inhibitor for metastatic uveal melanoma [abstract]. *Cancer Res.* **79** (Suppl. 13), CT068 (2019).
311. Onken, M. D. et al. Targeting nucleotide exchange to inhibit constitutively active G protein α subunits in cancer cells. *Sci. Signal.* **11**, eaao6852 (2018).
312. Ambrosini, G., Sawle, A. D., Musi, E. & Schwartz, G. K. BRD4-targeted therapy induces Myc-independent cytotoxicity in Gnaq/11-mutatant uveal melanoma cells. *Oncotarget* **6**, 33397–33409 (2015).
313. Chua, V. et al. Stromal fibroblast growth factor 2 reduces the efficacy of bromodomain inhibitors in uveal melanoma. *EMBO Mol. Med.* **11**, e9081 (2019).
314. Zimmer, L. et al. Phase II DeCOG-study of ipilimumab in pretreated and treatment-naïve patients with metastatic uveal melanoma. *PloS One* **10**, e0118564 (2015).
315. Joshua, A. M. et al. A phase 2 study of tremelimumab in patients with advanced uveal melanoma. *Melanoma Res.* **25**, 342–347 (2015).
316. Algazi, A. P. et al. Clinical outcomes in metastatic uveal melanoma treated with PD-1 and PD-L1 antibodies. *Cancer* **122**, 3344–3353 (2016).
317. Piulats, J. M. et al. Phase II multicenter, single arm, open label study of nivolumab (NIVO) in combination with ipilimumab (IPI) as first line in adult patients (pts) with metastatic uveal melanoma (MUM): GEM1402 NCT02626962 [abstract]. *J. Clin. Oncol.* **35** (Suppl. 15), 9533 (2017).
318. Damato, B. E., Dukes, J., Goodall, H. & Carvajal, R. D. Tebentafusp: T cell redirection for the treatment of metastatic uveal melanoma. *Cancers* **11**, E971 (2019).
319. Meijer, T. S. et al. Safety of percutaneous hepatic perfusion with melphalan in patients with unresectable liver metastases from ocular melanoma using the delcath systems' second-generation hemofiltration system: a prospective non-randomized phase II trial. *Cardiovasc. Intervent. Radiol.* **42**, 841–852 (2019).
320. Damato, B. et al. Patient-reported outcomes and quality of life after treatment of choroidal melanoma: a comparison of enucleation versus radiotherapy in 1596 patients. *Am. J. Ophthalmol.* **193**, 230–251 (2018).
This study evaluated the outcomes of different approaches to treat UM from the perspective of the patient.
321. Damato, B. et al. Patient-reported outcomes and quality of life after treatment for choroidal melanoma. *Ocul. Oncol. Pathol.* **5**, 402–411 (2019).
322. Afshar, A. R., Deiner, M., Allen, G. & Damato, B. E. The patient's experience of ocular melanoma in the US: a survey of the Ocular Melanoma Foundation. *Ocul. Oncol. Pathol.* **4**, 280–290 (2018).
323. Dogrusöz, M. et al. Differential expression of DNA repair genes in prognostically-favorable versus unfavorable uveal melanoma. *Cancers* **11**, E1104 (2019).
324. Doherty, R. E., Bryant, H. E., Valluru, M. K., Rennie, I. G. & Sisley, K. Increased non-homologous end joining makes DNA-PK a promising target for therapeutic intervention in uveal melanoma. *Cancers* **11**, E1278 (2019).
325. Zhang, B., Wu, H., Hao, J., Wu, Y. & Yang, B. Inhibition of DNA-PKcs activity re-sensitizes uveal melanoma cells to radio- and chemotherapy. *Biochem. Biophys. Res. Commun.* **522**, 639–646 (2020).
326. Ophthalmic Oncology Task Force. Local recurrence significantly increases the risk of metastatic uveal melanoma. *Ophthalmology* **123**, 86–91 (2016).
327. Davidorf, F. H. The melanoma controversy. A comparison of choroidal, cutaneous, and iris melanomas. *Surv. Ophthalmol.* **25**, 373–377 (1981).
328. Apt, L. Uveal melanomas in children and adolescents. *Int. Ophthalmol. Clin.* **2**, 403–410 (1962).
329. Shields, C. L. et al. Uveal melanoma in teenagers and children. A report of 40 cases. *Ophthalmology* **98**, 1662–1666 (1991).
330. Scholz, S. L. et al. Frequent *GNAQ, GNA11*, and *EIF1AX* mutations in iris melanoma. *Invest. Ophthalmol. Vis. Sci.* **58**, 3464–3470 (2017).
331. Krishna, Y. et al. Genetic findings in treatment-naïve and proton-beam-radiated iris melanomas. *Br. J. Ophthalmol.* **100**, 1012–1016 (2016).
332. van Poppelen, N. M. et al. Genetic background of iris melanomas and iris melanocytic tumors of uncertain malignant potential. *Ophthalmology* **125**, 904–912 (2018).
333. Harbour, J. W., Wilson, D., Finger, P. T., Worley, L. A. & Onken, M. D. Gene expressing profiling of iris melanomas. *Ophthalmology* **120**, 213–213.e3 (2013).
334. Shields, C. L. et al. Iris nevus growth into melanoma: analysis of 1611 consecutive eyes. *Ophthalmology* **120**, 766–772 (2013).
335. Shields, C. L. et al. Iris melanoma outcomes based on the American Joint Committee on Cancer classification (eighth edition) in 432 patients. *Ophthalmology* **125**, 913–923 (2018).
336. Popovic, M., Ahmed, I. I. K., DiGiovanni, J. & Shields, C. L. Radiotherapeutic and surgical management of iris melanoma: a review. *Surv. Ophthalmol.* **62**, 302–311 (2017).
337. Thariat, J. et al. Proton beam therapy for iris melanomas in 107 patients. *Ophthalmology* **125**, 606–614 (2018).
338. Gokhale, R., Medina, C. A., Biscotti, C. V. & Singh, A. D. Diagnostic fine-needle aspiration biopsy for iris melanoma. *Asia-Pac. J. Ophthalmol.* **4**, 89–91 (2015).
339. Petousis, V., Finger, P. T. & Milman, T. Anterior segment tumor biopsy using an aspiration cutter technique: clinical experience. *Am. J. Ophthalmol.* **152**, 771–775.e1 (2011).
340. Camp, D. A., Yadav, P., Dalvin, L. A. & Shields, C. L. Glaucoma secondary to intraocular tumors: mechanisms and management. *Curr. Opin. Ophthalmol.* **30**, 71–81 (2019).
341. Kaliki, S. & Shields, C. L. Focal Points 2015 Module: Choroidal Nevus. American Academy of Ophthalmology (2015).
342. Qiu, M. & Shields, C. L. Choroidal nevus in the United States adult population: racial disparities and associated factors in the National Health and Nutrition Examination Survey. *Ophthalmology* **122**, 2071–2083 (2015).
343. Kelland, L. R. "Of mice and men": values and liabilities of the athymic nude mouse model in anticancer drug development. *Eur. J. Cancer* **40**, 827–836 (2004).
344. Cao, J. & Jager, M. J. Animal eye models for uveal melanoma. *Ocul. Oncol. Pathol.* **1**, 141–150 (2015).
345. Braun, R. D. & Vistisen, K. S. Modeling human choroidal melanoma xenograft growth in immunocompromised rodents to assess treatment efficacy. *Invest. Ophthalmol. Vis. Sci.* **53**, 2693 (2012).
346. Gao, M., Tang, J., Liu, K., Yang, M. & Liu, H. Quantitative evaluation of vascular microcirculation using contrast-enhanced ultrasound imaging in rabbit models of choroidal melanoma. *Invest. Ophthalmol. Vis. Sci.* **59**, 1251 (2018).
347. Ent, Wvander et al. Modeling of human uveal melanoma in zebrafish xenograft embryos. *Invest. Ophthalmol. Vis. Sci.* **55**, 6612–6622 (2014).
348. Amirouchene-Angelozzi, N. et al. Establishment of novel cell lines recapitulating the genetic landscape of uveal melanoma and preclinical validation of mTOR as a therapeutic target. *Mol. Oncol.* **8**, 1508–1520 (2014).
349. Jager, M., Magner, J., Ksander, B. & Dubovy, S. Uveal melanoma cell lines: where do they come from? (an American Ophthalmological Society Thesis). *Trans. Am. Ophthalmol. Soc.* **114**, T5 (2016).
350. Siolas, D. & Hannon, G. J. Patient-derived tumor xenografts: transforming clinical samples into mouse models. *Cancer Res.* **73**, 5315–5319 (2013).
351. Hidalgo, M. et al. Patient-derived xenograft models: an emerging platform for translational cancer research. *Cancer Discov.* **4**, 998–1013 (2014).
352. Huang, J. L.-Y., Urtatiz, O. & Van Raamsdonk, C. D. Oncogenic G protein GNAQ induces uveal melanoma and intravasation in mice. *Cancer Res.* **75**, 3384–3397 (2015).
353. Perez, D. E., Henle, A. M., Amsterdam, A., Hagen, H. R. & Lees, J. A. Uveal melanoma driver mutations in GNAQ/11 yield numerous changes in melanocyte biology. *Pigment Cell Melanoma Res.* **31**, 604–613 (2018).
354. Moore, A. R. et al. GNA11 Q209L mouse model reveals RasGRP3 as an essential signaling node in uveal melanoma. *Cell Rep.* **22**, 2455–2468 (2018).
355. Ozaki, S. et al. Establishment and characterization of orthotopic mouse models for human uveal melanoma hepatic colonization. *Am. J. Pathol.* **186**, 43–56 (2016).
356. Folberg, R. et al. Modeling the behavior of uveal melanoma in the liver. *Invest. Ophthalmol. Vis. Sci.* **48**, 2967–2974 (2007).
357. Papakostas, T. D., Lane, A. M., Morrison, M., Gragoudas, E. S. & Kim, I. K. Long-term outcomes after proton beam irradiation in patients with large choroidal melanomas. *JAMA Ophthalmol.* **135**, 1191–1196 (2017).
358. Furdova, A. et al. Clinical experience of stereotactic radiosurgery at a linear accelerator for intraocular melanoma. *Melanoma Res.* **27**, 463–468 (2017).
359. Wackernagel, W. et al. Local tumour control and eye preservation after gamma-knife radiosurgery of choroidal melanomas. *Br. J. Ophthalmol.* **98**, 218–223 (2014).
360. Blasi, M. A. et al. Photodynamic therapy in ocular oncology. *Biomedicines* **6**, 17 (2018).
361. Fabian, I. D. et al. Primary photodynamic therapy with verteporfin for pigmented posterior pole cT1a choroidal melanoma: a 3-year retrospective analysis. *Br. J. Ophthalmol.* **102**, 1705–1710 (2018).
362. Cassoux, N. et al. Choroidal melanoma: does endoresection prevent neovascular glaucoma in patient treated with proton beam irradiation? *Retina* **33**, 1441–1447 (2013).
363. Brovkina, A. F. Local treatment of choroidal melanoma: possibilities and limitations. *Vestn. Oftalmol.* **134**, 52–60 (2018).
364. Rice, J. C. et al. Brachytherapy and endoresection for choroidal melanoma: a cohort study. *Br. J. Ophthalmol.* **98**, 86–91 (2014).
365. Vidoris, A. A. C. et al. Outcomes of primary endoresection for choroidal melanoma. *Int. J. Retina Vitr.* **3**, 42 (2017).
366. Hirobe, T., Ito, S. & Wakamatsu, K. The mouse pink-eyed dilution allele of the P-gene greatly inhibits eumelanin but not pheomelanin synthesis: the pink-eyed dilution gene and melanin. *Pigment. Cell Melanoma Res.* **24**, 241–246 (2011).
367. Pellosi, M. C. et al. Effects of the melanin precursor 5,6-dihydroxy-indole-2-carboxylic acid (DHICA) on DNA damage and repair in the presence of reactive oxygen species. *Arch. Biochem. Biophys.* **557**, 55–64 (2014).
368. Rogers, M. S. et al. The classical pink-eyed dilution mutation affects angiogenic responsiveness. *PLoS One* **7**, e35237 (2012).
369. Wakamatsu, K., Hirobe, T. & Ito, S. High levels of melanin-related metabolites in plasma from pink-eyed dilution mice. *Pigment Cell Res.* **20**, 222–224 (2007).
370. Vivet-Noguer, R., Tarin, M., Roman-Roman, S. & Alsafadi, S. Emerging therapeutic opportunities based on current knowledge of uveal melanoma biology. *Cancers* **11**, E1019 (2019).
371. Grossniklaus, H. E. Understanding uveal melanoma metastasis to the liver: the Zimmerman effect and the Zimmerman hypothesis. *Ophthalmology* **126**, 483–487 (2019).

Acknowledgements
The Horizon 2020 grant 667787, UM CURE, helped to build international collaborations (M.J.J. and M.-H.S.).

Author contributions
Introduction (M.J.J., C.L.S., C.M.C., M.H.A.-R., H.E.G., M.-H.S., R.D.C., R.J. and B.E.D.); Epidemiology (M.J.J., C.M.C., M.H.A.-R., H.E.G., R.N.B., R.J. and B.E.D.); Mechanisms/pathophysiology (M.J.J., C.M.C., M.H.A.-R., H.E.G., M.-H.S., R.D.C. and R.J.); Diagnosis, screening and prevention (M.J.J., C.L.S., R.D.C., R.N.B., J.A.S. and B.E.D.); Management (C.L.S., R.D.C., J.A.S. and B.E.D.); Quality of life (R.D.C. and B.E.D.); Outlook (M.J.J., C.L.S., H.E.G., R.J. and B.E.D.); Overview of the Primer (M.J.J.).

Competing interests
C.L.S. is a Member of the Scientific Advisory board of Aura Biosciences, Inc. B.E.D. is a part-time consultant for AURA Biosciences Inc., Cambridge Biosciences and Immunocore Ltd. The remaining authors declare no competing interests.

Peer review information
Nature Reviews Disease Primers thanks M. A. Blasi, U. Keilholz, J. Niederkorn, J. Pe'er, U. Pfeffer, K. Sisley, and the other, anonymous, reviewer(s) for their contribution to the peer review of this work.

Publisher's note
Springer Nature remains neutral with regard to jurisdictional claims in published maps and institutional affiliations.

RELATED LINKS
Liverpool Uveal Melanoma Prognosticator Online: www.lumpo.net
Oculonco: www.oculonco.com
Uveal Melanoma TNM Staging and Survivorship: www.ocularmelanomaonline.org